Article

Current Biology

Miniature linear and split-belt treadmills reveal mechanisms of adaptive motor control in walking *Drosophila*

Graphical abstract

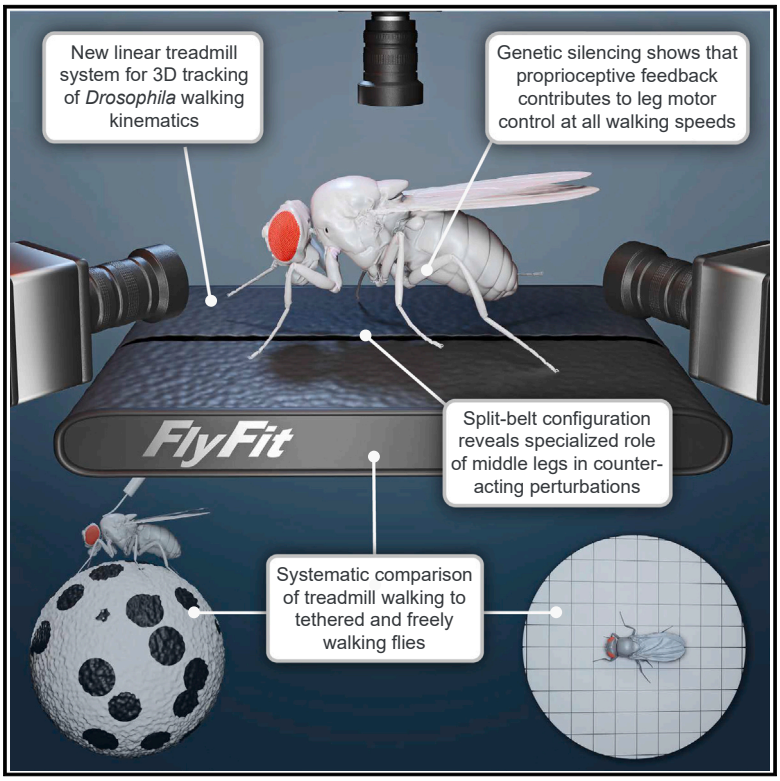

Highlights

- A new actuated treadmill system captures 3D kinematics of flies compelled to walk
- Flies walking on the treadmill have similar kinematics to freely walking flies
- Proprioceptive feedback is important for leg motor control at all walking speeds
- Flies on a split-belt treadmill use their middle legs to counteract perturbations

Authors

Brandon G. Pratt, Su-Yee J. Lee, Grant M. Chou, John C. Tuthill

Correspondence

tuthill@uw.edu

In brief

Pratt et al. engineer tiny treadmills that enable 3D tracking of fruit fly walking kinematics. The authors systematically compare treadmills to free and tethered walking, evaluate the role of proprioceptive feedback across walking speeds, and reveal how flies adapt their stepping patterns to maintain course on a split-belt treadmill.

Pratt et al., 2024, Current Biology *34*, 1–14
October 7, 2024
https://doi.org/10.1016/j.cub.2024.08.006

CellPress

Please cite this article in press as: Pratt et al., Miniature linear and split-belt treadmills reveal mechanisms of adaptive motor control in walking *Drosophila*, Current Biology (2024), https://doi.org/10.1016/j.cub.2024.08.006

Current Biology

CellPress

Article

Miniature linear and split-belt treadmills reveal mechanisms of adaptive motor control in walking *Drosophila*

Brandon G. Pratt,[1] Su-Yee J. Lee,[1] Grant M. Chou,[1] and John C. Tuthill[1,2,*]
[1]Department of Physiology and Biophysics, University of Washington, Seattle, WA 98195, USA
[2]Lead contact
*Correspondence: tuthill@uw.edu
https://doi.org/10.1016/j.cub.2024.08.006

SUMMARY

To navigate complex environments, walking animals must detect and overcome unexpected perturbations. One technical challenge when investigating adaptive locomotion is measuring behavioral responses to precise perturbations during naturalistic walking; another is that manipulating neural activity in sensorimotor circuits often reduces spontaneous locomotion. To overcome these obstacles, we introduce miniature treadmill systems for coercing locomotion and tracking 3D kinematics of walking *Drosophila*. By systematically comparing walking in three experimental setups, we show that flies compelled to walk on the linear treadmill have similar stepping kinematics to freely walking flies, while kinematics of tethered walking flies are subtly different. Genetically silencing mechanosensory neurons altered step kinematics of flies walking on the linear treadmill across all speeds. We also discovered that flies can maintain a forward heading on a split-belt treadmill by specifically adapting the step distance of their middle legs. These findings suggest that proprioceptive feedback contributes to leg motor control irrespective of walking speed and that the fly's middle legs play a specialized role in stabilizing locomotion.

INTRODUCTION

Many animals rely on legged locomotion to move through diverse and unpredictable environments. To accomplish behavioral goals in the face of this unpredictability, nervous systems have evolved to control the body in an adaptive manner. Animals as diverse as cockroaches[1] and humans[2] use similar strategies to recover from unexpected motor outcomes (e.g., tripping) by rapidly adjusting coordination within and between legs. Understanding how sensorimotor neural circuits detect perturbations and generate adaptive motor responses remains a fundamental problem in neuroscience.[3]

A common method to investigate the neural control of movement is to perturb neurons within candidate circuits and measure the effect on an animal's behavior. For example, past efforts to identify sensorimotor circuits have relied on anatomical lesions.[4,5] While these methods revealed regions of the nervous system that are important for proprioceptive sensing and motor control, they lack cell-type specificity and produce wide-ranging behavioral effects. More recently, genetic methods have enabled targeted manipulation of specific cell types that sense or control the body. However, these experimental manipulations often decrease the probability and vigor of spontaneous behavior. For example, the loss of feedback from mechanosensory neurons in both mammals[6] and insects[7] reduces walking speed and probability. This confound has made it challenging to dissect the relative roles of mechanosensory feedback versus feedforward motor commands across different walking speeds.[8]

One strategy to overcome this reduction in spontaneous behavior is to compel animals to walk, for example, by placing them on an actuated treadmill. Treadmills have been historically used to study the neural basis of motor control and adaptive locomotion in both vertebrates[9–11] and invertebrates.[12–17] For instance, treadmills have been used to drive walking in cats[18] and rodents,[19] leading to important insights into spinal circuits for adaptive locomotor control.

Because treadmills are externally controlled, they can also deliver calibrated mechanical perturbations to walking animals. Previous work showed that cats walking on a treadmill learn to increase the height of their steps to avoid being smacked by a paddle.[20] Split-belt treadmills, which consist of two independently controlled belts, are another classic paradigm to investigate walking coordination and motor adaptation. Both humans[21–23] and mice[24] adopt new inter-leg coordination patterns when their left and right legs are driven at different speeds on a split-belt treadmill. This phenomenon of split-belt adaptation has been used to investigate behavioral and neural mechanisms of adaptive locomotion.[25] A final advantage of treadmills is that they enable the study of locomotion within a confined space, which is important for capturing body kinematics or physiological signals from neurons and muscles. For example, one trailblazing study recorded leg joint kinematics and muscle activity in rock lobsters walking on a split-belt treadmill.[26]

In recent years, the fruit fly, *Drosophila melanogaster*, has emerged as an important model system for studying

Please cite this article in press as: Pratt et al., Miniature linear and split-belt treadmills reveal mechanisms of adaptive motor control in walking *Drosophila*, Current Biology (2024), https://doi.org/10.1016/j.cub.2024.08.006

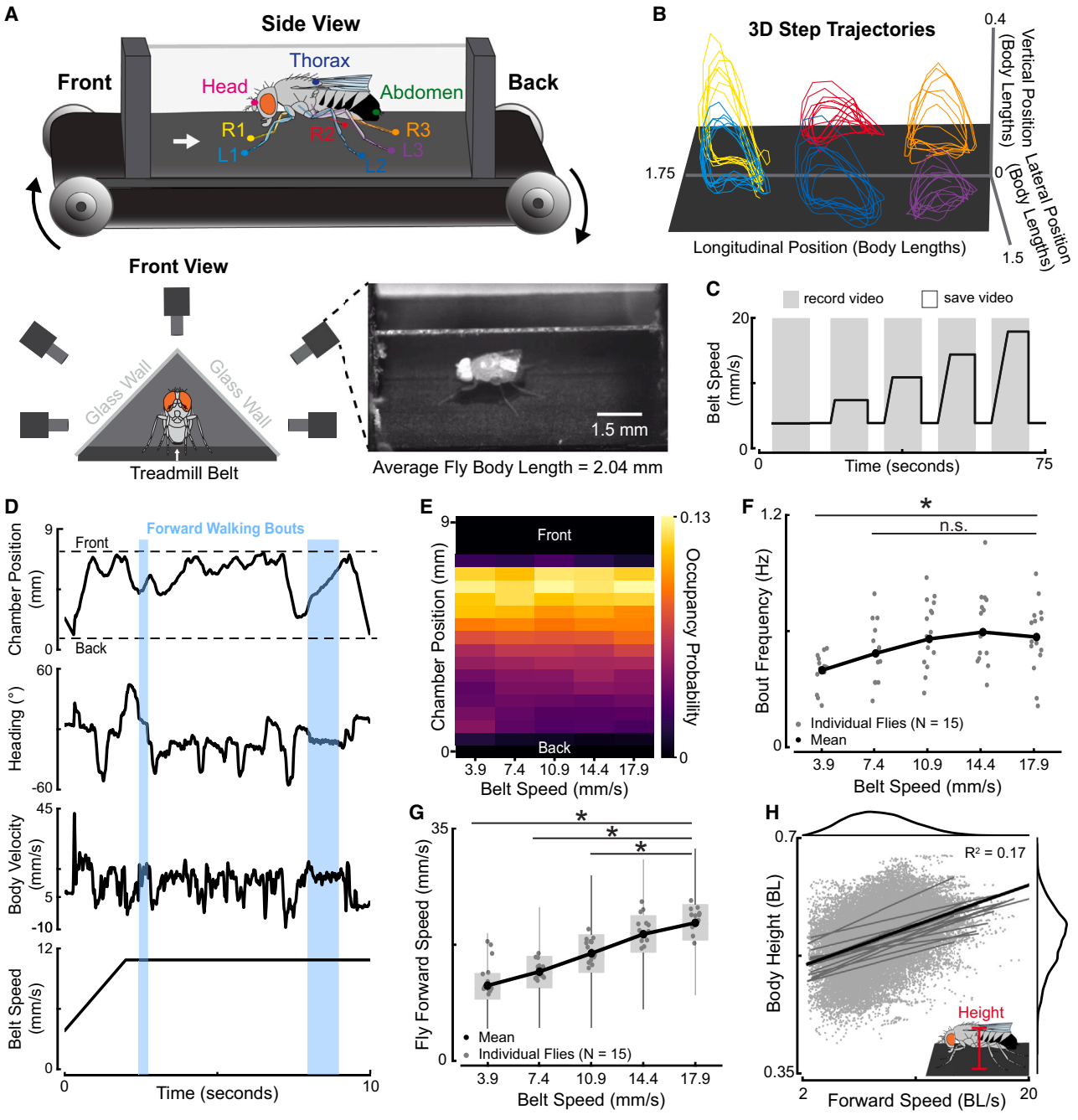

Figure 1. The linear treadmill controls locomotor speed and enables tracking of 3D kinematics in walking *Drosophila*

(A) Schematic of the linear treadmill setup. Key points associated with the head, thorax, abdomen, and each leg tip were tracked in 3D. Flies were recorded with 5 high-speed cameras as they were driven to walk on the treadmill within an attic-shaped chamber. Flies had an average body length of 2.04 ± 0.10 mm. Note that the schematic flies are not to scale.

(B) 3D leg tip (tarsi) trajectories during forward walking. Colors correspond to the labels in (A).

(C) Flies were compelled to walk by moving the treadmill belt at one of 5 steady-state speeds. Each speed was presented to a fly 10 times, with speeds randomly interleaved. Each trial was composed of a 10 s recording period (gray) followed by a 5 s saving period (white).

(D) A representative trial of a fly walking on the treadmill with a belt speed of 10.9 mm/s. The position of the fly along the chamber (measured at the thorax), the fly's heading angle and body velocity, and the belt speed profile are plotted from top to bottom, respectively. Forward walking bouts (see STAR Methods for classification) are highlighted by the light blue shaded regions.

(E) Flies walked between the middle and front of the chamber across all belt speeds.

(F) Flies increased their walking bout frequency as the belt speed increased. A t test on the mean bout frequency across flies was used to determine statistical significance (*$p < 0.05$). The edges of the horizontal black lines indicate which two groups were statistically compared. Gray dots are the mean frequency of individual flies, while the black line denotes the mean across all flies.

(legend continued on next page)

Please cite this article in press as: Pratt et al., Miniature linear and split-belt treadmills reveal mechanisms of adaptive motor control in walking *Drosophila*, Current Biology (2024), https://doi.org/10.1016/j.cub.2024.08.006

proprioceptive sensing and adaptive locomotion.[7,27–32] The key advantages of the fly are a compact, fully mapped nervous system[33–35] and cell-type-specific tools for targeted genetic manipulations. Fly locomotion has been previously studied in tethered animals walking on a floating sphere[36–39] or in freely walking animals constrained to a behavioral arena.[7,40–44] One advantage of the tethered preparation is that it enables 3D tracking of the fly's body and legs,[45,46] which has not previously been possible in freely walking flies. It is also possible to record neural signals of tethered flies using optical imaging[47] or electrophysiology.[48,49] However, one disadvantage of studying locomotion in tethered flies is that their posture is constrained and normal ground reaction forces may be disrupted, which could affect walking kinematics.

To bridge these established methodologies, we introduce a new linear treadmill system that enables long-term 3D tracking of walking *Drosophila*. We systematically compare walking kinematics on the linear treadmill to those of freely walking and tethered flies. We then use the linear treadmill to investigate step kinematics and inter-leg coordination following genetic silencing of mechanosensory neurons. Last, we introduce a novel split-belt treadmill for fruit flies, which we use to uncover behavioral mechanisms of adaptive motor control. We provide open-source software and hardware designs for these treadmill systems as resources for the community.

RESULTS

A linear treadmill for tracking 3D walking behavior in *Drosophila*

We engineered a miniature linear treadmill system to measure 3D walking kinematics in flies (Figure 1A). A fly was constrained to walk on the treadmill within a transparent chamber, and its wings were trimmed to discourage flight initiation. (We note that flies did not walk on the treadmill while tethered; see STAR Methods for more details.) We used 5 high-speed video cameras (180 fps) to record fly walking behavior. To test the treadmill system, we used wild-type Berlin flies that had a body length (BL) of 2.04 ± 0.10 mm. We used DeepLabCut[50] and Anipose[46] to track and extract 3D kinematics of the fly leg tips and body (Figure 1B).

We first measured the 3D kinematics of flies as they walked across a range of belt driving speeds (Figure 1C). As illustrated by a representative fly walking at an intermediate belt speed (Figure 1D; Video S1), flies on the treadmill displayed forward walking bouts, standing, and other lateral movements. Flies traversed the entirety of the chamber but spent most of their time toward the front (Figure 1E). They typically walked in short bursts, accelerating toward the front of the chamber, where they would walk for a short period, after which they would ride the belt to the back of the chamber; contact with the back of the chamber would then initiate another walking bout. Flies increased their walking bout frequency as the belt speed increased, which we quantified using the frequency at which they crossed the middle of the chamber from the rear (Figure 1F). The sporadic structure of fly treadmill walking resembles that previously reported for freely walking flies.[51]

Flies on the treadmill also consistently increased their walking speed to keep up with the treadmill's belt driving speed (Figure 1G). At the extremes, flies on the treadmill were able to sustain walking at a max belt speed of 40 mm/s (Video S2) and surpassed an instantaneous walking velocity of 50 mm/s (Video S3), which is the fastest walking speed ever reported for *Drosophila melanogaster*. By driving flies to walk across a range of speeds while recording their 3D kinematics, we found that flies increased their body height as they walked faster by 0.007 BL per second (BL/s) (Figure 1H). Note that we converted mm to BLs when appropriate to normalize for natural variation in fly size.

In summary, our engineered treadmill makes it possible to force individual flies to walk for long periods (up to 1 h), while tracking 3D body and leg kinematics. Based on a behavioral classifier and the smoothed instantaneous body velocity, flies remained upright 97% of the time on the treadmill and spent an average of 54% of the time walking (28% of which consisted of straight forward walking compared with non-straight walking), enabling collection of large amounts of useful kinematic data from each animal despite their sporadic natural walking behavior. Consistent with prior work in freely walking flies,[52] we found that flies on the treadmill elevate their body as they walked faster, a relationship that has also been found in many other walking animals, from cockroaches[53] to humans.[54]

Comparison of walking kinematics between treadmill, freely, and tethered walking flies

Previous studies have quantified step kinematics of freely walking flies.[7,40,41,43,52,55,56] To compare treadmill walking to freely walking kinematics, we collected and analyzed a new dataset of wild-type flies freely walking in the commonly used fly bowl arena.[42] We focused our kinematic analyses on walking bouts in which flies had a stable forward heading, identified based on fly heading direction and body velocity (examples in Figure 1D; see STAR Methods for details). We chose to focus on these forward walking bouts because they are comparable to flies walking against the driving axis of the treadmill. Note that walking parameters were only calculated for periods where flies on the treadmill walked in the middle of the chamber because flies displayed reaching behaviors at the front of the chamber (i.e., tried to grab onto the chamber). At the back of the chamber, the fly's legs were occasionally obscured. By restricting our analysis to the middle of the chamber, we could be confident that leg kinematics were tracked with high fidelity and not contaminated by leg movements other than walking.

(G) Flies increased their forward walking speed as the belt speed increased. A Kruskal-Wallis test on the median forward speed across flies was used to determine statistical significance (*$p < 0.05$). The edges of the horizontal black lines indicate which two groups were statistically compared. Boxplots (box, 25th–75th percentile; whiskers, 1.5 IQR from lower and upper quartiles) show the distribution of pooled data. Black line connects the mean forward speed across all flies and belt speeds.

(H) Flies increased their body height (vertical distance between the thorax and ground) as they walked faster (in body lengths per second, or BL/s). Black, population fit; gray line, individual fit. R^2 was computed from the population fit.

See also Videos S1, S2, and S3.

Please cite this article in press as: Pratt et al., Miniature linear and split-belt treadmills reveal mechanisms of adaptive motor control in walking *Drosophila*, Current Biology (2024), https://doi.org/10.1016/j.cub.2024.08.006

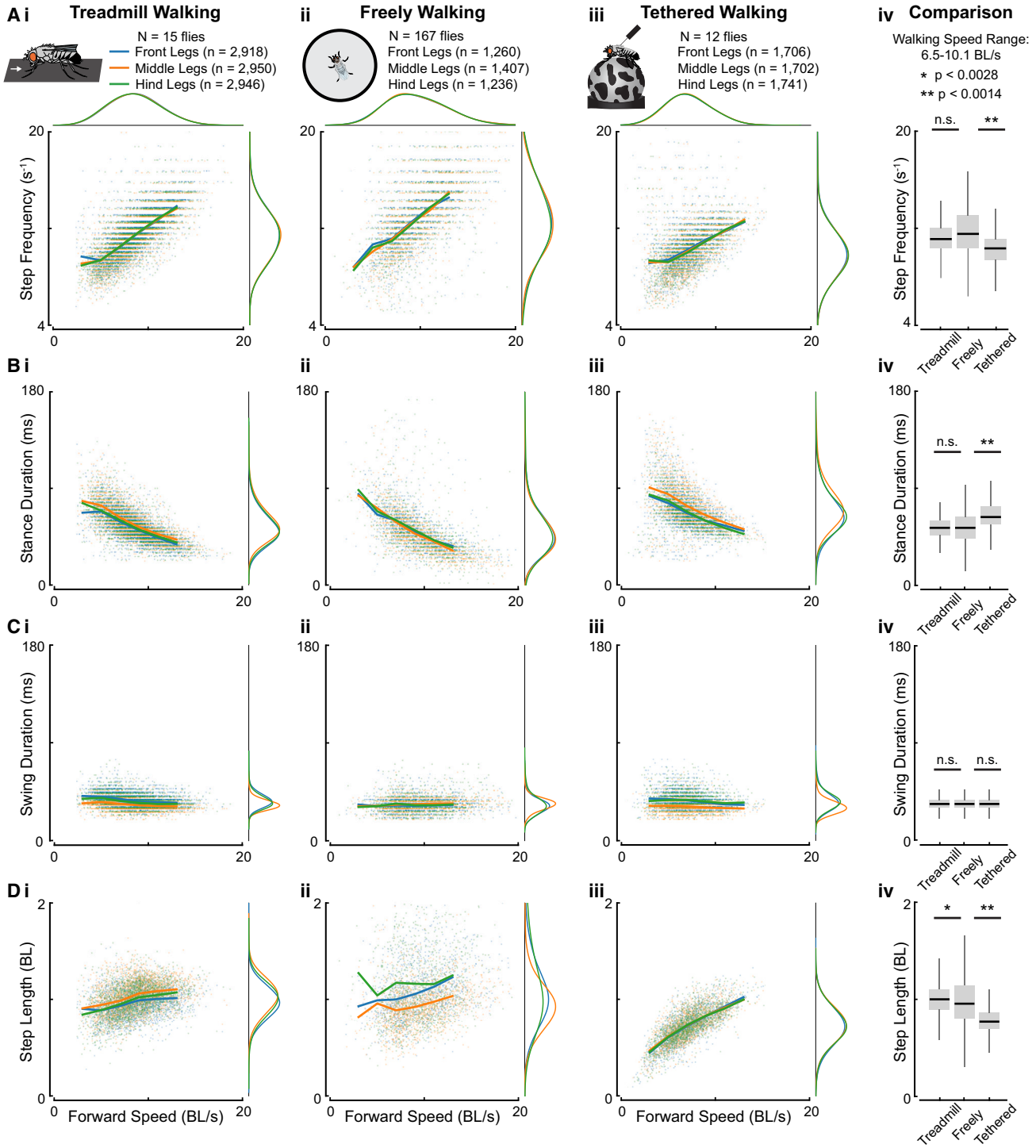

Figure 2. Step kinematics are similar across treadmill and freely walking flies but subtly different from tethered flies

(A) Step frequency of the front (blue), middle (orange), and hind (green) legs as a function of forward walking speed for treadmill (Ai), freely walking (Aii), and tethered flies (Aiii). Distributions (Aiv; gray boxplots) that combine step frequency across leg pairs for treadmill, freely, and tethered walking flies over an overlapping and dense range of walking speeds (6.5–10.1 BL/s).

(B) Stance duration as a function of forward walking speed for flies in the different setups.

(C) Swing duration as a function of forward walking speed.

(D) Step length as a function of forward walking speed.

Lines are speed-binned averages (2 BL/s bins between 3 and 13 BL/s) for each kinematic parameter and leg pair. Step frequency, stance duration, and swing duration (A–C) were computed on interpolated data for treadmill (Di; 180–300 fps) and freely walking flies (Dii; 150–300 fps) to enable the comparison to tethered

(legend continued on next page)

Please cite this article in press as: Pratt et al., Miniature linear and split-belt treadmills reveal mechanisms of adaptive motor control in walking *Drosophila*, Current Biology (2024), https://doi.org/10.1016/j.cub.2024.08.006

We found that the key relationships between stepping kinematics and forward walking speed were similar between flies walking on the treadmill (Figure 2i) and freely walking flies (Figure 2ii; Video S4) (a glossary containing definitions of kinematic parameters can be found in the STAR Methods). Flies in both setups increased step frequency as they walked faster (Figures 2Ai and 2Aii). Correspondingly, stance duration was inversely related to walking speed for flies in both setups (Figures 2Bi and 2Bii). However, swing duration remained fairly constant across speeds and had a similar magnitude for treadmill and freely walking flies (Figures 2Ci and 2Cii). Step length, the distance between the footfalls of each leg, was also comparable between treadmill and freely walking flies (Figures 2Di and 2Dii). Flies in both setups had similar increases in step length with increasing walking speed.

The largest difference between treadmill and freely walking flies was that the step kinematics of freely walking flies were more variable (step frequency within the walking speed range of 6.5–10.1 BL/s: freely walking, $\sigma^2 = 5.18\ s^{-1}$; treadmill walking, $\sigma^2 = 1.98\ s^{-1}$). The step kinematics of freely walking flies may have been more variable because they were walking on a slightly sloped surface in the fly bowl (11°), and slope angle has been shown to influence fly walking kinematics.[57] Flies on the treadmill walked against a single driving axis at a prescribed speed, which may have produced straighter walking bouts, more symmetric speed distributions, and less variable step kinematics. The step kinematics of flies in our freely walking dataset were also consistent with prior work,[7,40,43,55,56] even though fly strain and sex were often different in those studies (Table S1). Overall, the step kinematics of flies walking on the treadmill were similar to freely walking flies.

Having developed a framework for comparing walking kinematics across experimental setups, we took the opportunity to extend our analysis to a third setup: tethered flies walking on a floating sphere (Figure 2iii; Video S5). The "fly-on-a-ball" setup is commonly used in our lab[27,46,58] and many others,[36,38,47] but leg kinematics of tethered and freely walking flies have not been systematically compared.

In general, we found that the relationships between stepping kinematics and walking speed were similar across all three setups. However, tethered flies differed from untethered ones (i.e., treadmill and freely walking flies) in several key aspects. First, tethered flies did not reach the faster walking speeds displayed by untethered flies. By restricting our analysis to the speed range of 6.5–10.1 BL/s to account for the slower walking of tethered flies, we found that the step frequency of tethered flies was also significantly lower than that of untethered flies (Figure 2Aiv), whereas stance duration was significantly longer (Figure 2Biv). There was not a significant difference in swing duration across the three setups (Figure 2Civ). Therefore, the reduced step frequency in tethered flies appears to be produced by longer stance durations across walking speeds.

Tethered flies also had a significantly lower step length than untethered flies (Figure 2Div). However, the step length of tethered flies was more correlated with walking speed (tethered, r = 0.41; freely, r = 0.05; treadmill, r = 0.22). We also examined each of these step kinematic parameters over narrower speed ranges and found similar kinematic relationships at intermediate and fast walking speeds (Figures S1A–S1D). Step frequency and step length were significantly different across all setups at slow walking speeds, whereas stance duration was not significantly different. A likely reason for the differences at slower walking speeds compared with faster ones is that step kinematics tend to be more variable at slower walking speeds.[7,40]

In addition to these pairwise kinematic comparisons, we used a similarity metric based on KL divergence to ask whether freely walking kinematics were more similar to those obtained from tethered or freely walking flies (Figures S1E–S1H). We found that there was a greater similarity in the step kinematics between treadmill and freely walking flies, especially at fast walking speeds. These differences in step kinematics and walking speed ranges between tethered and untethered flies may be because the tethered flies are walking on a spherical surface and/or because their body weight is supported by a rigid tether.

We next compared inter-leg coordination parameters during forward straight walking bouts across the three setups. We quantified the number of legs that were in the stance phase of the step cycle at each point in time, a metric that remains constant for idealized coordination patterns such as the tripod pattern, in which 3 legs alternate between stance and swing.[40] We found that the probability of having a specific number of legs in stance was similar between tethered and untethered flies. Specifically, flies in all three setups showed an increased probability of having 3 legs in stance as walking speed increased (Figure 3A). This is consistent with prior work showing that freely walking flies are more likely to use a canonical tripod coordination pattern at higher speeds.[7,40,56,59]

Given that flies across all three setups had similar speed-dependent changes in inter-leg coordination, we next asked if the stepping pattern underlying inter-leg coordination was different between tethered and untethered flies. We therefore examined the relative swing and stance relationships across legs. We observed that the order in which legs entered stance conformed to the so-called *Cruse Control* rules[8,60,61] for both tethered and untethered flies. This is illustrated by the anterior progression of ipsilateral leg stepping (diagonal black stripes in Figure 3B).

We also examined the relative phase relationships between the left front leg and all other legs across the different setups. Phase was computed by determining when a leg entered stance within the left front leg's step cycle. Surprisingly, we found different relative phase relationships between flies walking on the treadmill and those walking in the other setups (Figure 3C). Freely walking flies, for example, had more variable phase

flies. The scatterplots for each walking setup were slightly offset in (A)–(C) so that each could be visually distinct. Marginal distributions were computed on the original, non-offset distributions. In (A)–(Civ), chi-squared test for goodness of fit with a Bonferroni correction was used to statistically compare the distribution of freely walking flies to that of each other setup. In (D), a t test with a Bonferroni correction was used to compare the distribution of freely walking flies to that of each other setup. *N*, number of flies; *n*, number of steps. See also Figure S1 for comparisons of the similarity between the setups with respect to step kinematics, leg pairs, and walking speeds.
See also Figure S1 and Videos S4 and S5.

Please cite this article in press as: Pratt et al., Miniature linear and split-belt treadmills reveal mechanisms of adaptive motor control in walking *Drosophila*, Current Biology (2024), https://doi.org/10.1016/j.cub.2024.08.006

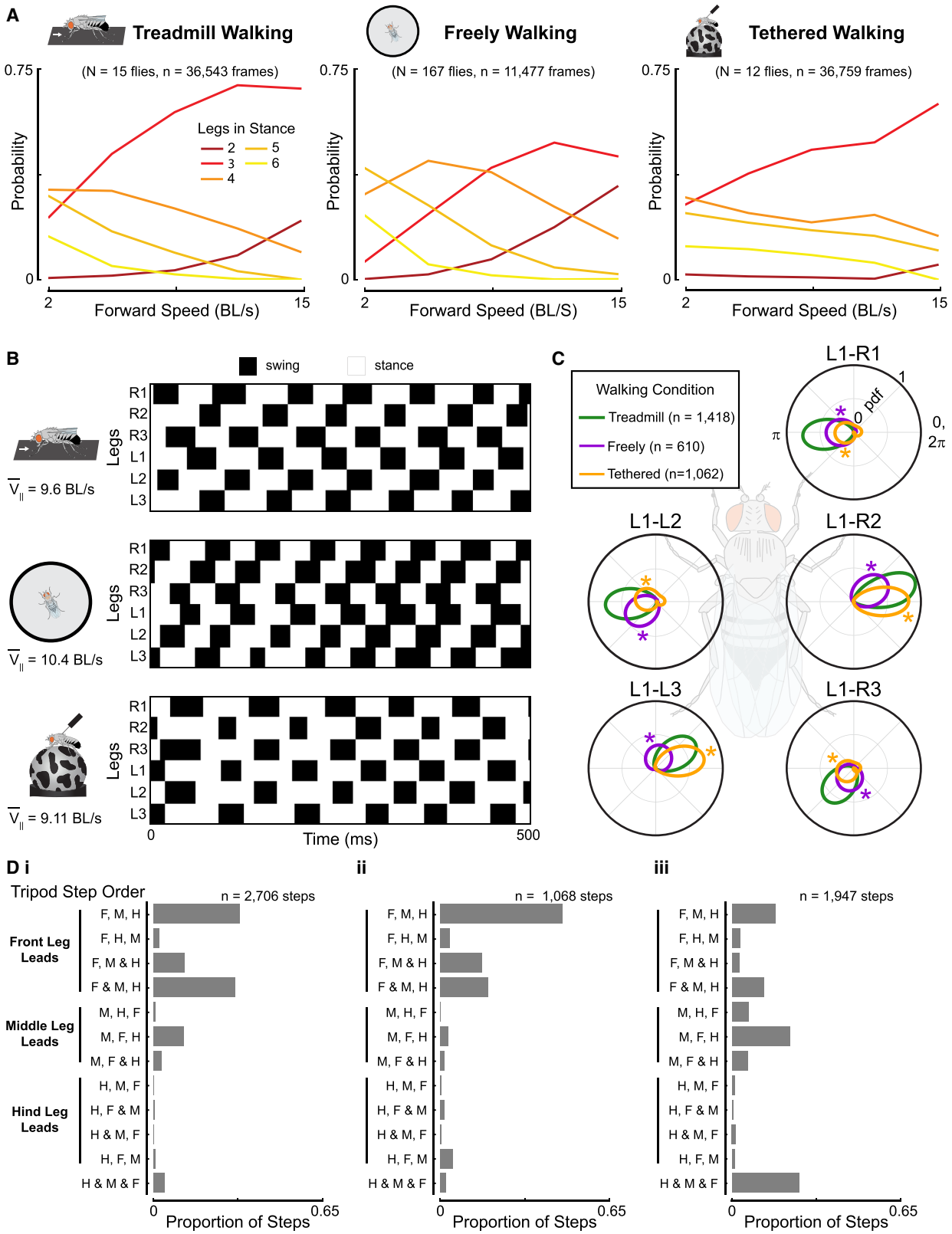

Figure 3. Subtle differences in inter-leg coordination between tethered and untethered flies

(A) Probability of treadmill, freely walking, and tethered flies exhibiting 2–6 legs in stance in each video frame across forward walking speeds. Lines are speed-binned averages of the probability of a certain number of legs in stance (3.2 BL/s bins between 2 and 15 BL/s). *N*, number of flies; *n*, number of video frames.

(legend continued on next page)

Please cite this article in press as: Pratt et al., Miniature linear and split-belt treadmills reveal mechanisms of adaptive motor control in walking *Drosophila*, Current Biology (2024), https://doi.org/10.1016/j.cub.2024.08.006

relationships (i.e., a wider distribution) and a peak probability density at a different phase compared with flies walking on the treadmill. Like with step kinematics, the inter-leg coordination of freely walking flies may be more variable because they walked on a slightly sloped surface. The peak probability of the relative phase relationships was also significantly different for tethered flies compared with flies walking on the treadmill. In particular, the phase relationships of the ipsilateral front/hindlegs and contralateral middle leg that make up the canonical tripod were more coupled for tethered flies; that is, their peak probability densities were centered around 0 or π. However, we note that the average phase relationships of flies in all setups resembled the canonical tripod coordination pattern.

Finally, we looked at the order in which legs within a tripod entered stance with respect to the left front leg's step cycle. We found differences in the stance onset order between tethered and untethered flies. For example, the front leg within a tripod was usually the first leg to contact the ground for treadmill (Figure 3Di) and freely walking flies (Figure 3Dii), whereas the stance order was more variable for tethered flies; for example, tethered flies had more instances of the middle leg entering stance first (Figure 3Diii). Tethered flies also had more instances where all legs within a tripod entered stance at the same time, called an "ideal tripod." Therefore, the inter-leg phase coupling of tethered flies was stronger than that of untethered flies. One explanation could be that the added stability from the tether induces a more tightly coupled inter-leg coordination pattern. In summary, we found that although step kinematics were subtly different between tethered and untethered flies (Figure 2), inter-leg coordination was broadly similar (Figure 3).

Silencing mechanosensory feedback alters step kinematics across walking speeds and not inter-leg coordination

One of our motivations to develop a linear treadmill was to investigate the role of mechanosensory feedback in fly locomotion. This has historically been challenging because silencing mechanosensory neurons typically leads to a reduction in locomotor probability and speed in flies[7] and other animals.[5,6] To test whether flies lacking mechanosensory feedback walk on the linear treadmill, we genetically silenced chordotonal neurons (iav-GAL4 > UAS-kir2.1; see table in STAR Methods for full genotype), which are found at multiple joints throughout the fly's body, including in the femoral chordotonal organ (Figure 4A). As expected, silencing chordotonal neurons drastically reduced locomotion in freely walking flies; however, the linear treadmill was able to drive mechanosensory-deficient flies to walk for a greater proportion of time (Figure 4B). Moreover, these flies increased their walking speed as the belt speed increased (Figure 4C), allowing us to characterize kinematics across a wide range of walking speeds. Silencing chordotonal neurons altered the structure of fly locomotion on the treadmill compared with genetically matched UAS-Kir 2.1 and iav-GAL4 controls (see table in STAR Methods for full genotype). Compared with controls, flies with silenced chordotonal neurons spent more time at the back of the chamber, especially at fast belt speeds (Figure 4D). Flies with silenced chordotonal neurons also had a higher walking bout frequency than controls (Figure 4E). Altogether, flies lacking chordotonal neuron feedback were capable of walking at fast speeds on the treadmill, but their overall walking behavior was altered compared with controls.

The leg movements of flies with silenced chordotonal neurons were noticeably different. Qualitatively, the legs appeared less rigid and moved with less precision (Video S6). Therefore, we next analyzed the impact of silencing chordotonal neurons on step kinematics and inter-leg coordination during forward, straight walking bouts. We found that flies lacking chordotonal feedback had a lower step frequency across legs and speeds compared with control flies (Figure 4F). Interestingly, the step frequency of the front legs was less altered at slower walking speeds compared with the other legs. This could be because the front legs may be specialized for steering the animal,[30] whereas the other legs are also involved in body propulsion.[62] In addition to step frequency, flies with silenced chordotonal neurons had greater step lengths across speeds, suggesting that they increased the size of their steps to compensate for taking fewer of them (Figure 4G). We also found some differences in inter-leg coordination, as measured by relative phase (Figure 4H). However, we also observed differences in inter-leg coordination between the two control genotypes. Variation in walking kinematics of flies from different genetic backgrounds is consistent with past work showing that different wild-type strains exhibit different speed-dependent inter-leg coordination patterns and step kinematics.[56] Overall, silencing chordotonal neurons led to clear impairments in step kinematics across walking speeds, but the impact on inter-leg coordination was less clear.

To demonstrate that the treadmill system is also able to detect kinematic changes following more specific genetic manipulations, we also tested a second genotype that labels a combination of different leg proprioceptors, including campaniform sensilla and hair plate neurons (Figure S2). Expressing Kir 2.1 with this driver line produced deficits in step kinematics and inter-leg coordination that were similar to the chordotonal neuron manipulations. The larger step lengths and lower step frequencies of flies with altered proprioceptive feedback are consistent with previous studies that used broad driver lines labeling many mechanosensory neurons[7] or chordotonal neurons labeled by the iav-GAL4 driver line.[29] In summary, these results demonstrate the advantage of the linear treadmill in investigating the role of sensory feedback in locomotion.

(B) Representative plots of the swing and stance phases of each leg across all setups. Black, swing; white, stance.
(C) Polar plots of the relative phase between the left front leg and each other leg for flies in each setup. Kernel density estimations were used to determine the probability density functions. Each PDF integrates to 1. A two-sample Kuiper test with a Bonferroni correction was used to statistically compare the population distributions of treadmill and freely walking flies (purple) and treadmill and tethered walking flies (orange) (*$p < 0.003$; *n*, number of phase comparisons).
(D) Proportion of steps attributed to each step order combination of the legs with a tripod for treadmill (Di), freely (Dii), and tethered (Diii) walking flies. The leading leg is indicated on the left of the graph; "&" denotes legs contacting the ground at the same time; *n*, number of steps.
See also Figure S1 and Videos S4 and S5.

Please cite this article in press as: Pratt et al., Miniature linear and split-belt treadmills reveal mechanisms of adaptive motor control in walking *Drosophila*, Current Biology (2024), https://doi.org/10.1016/j.cub.2024.08.006

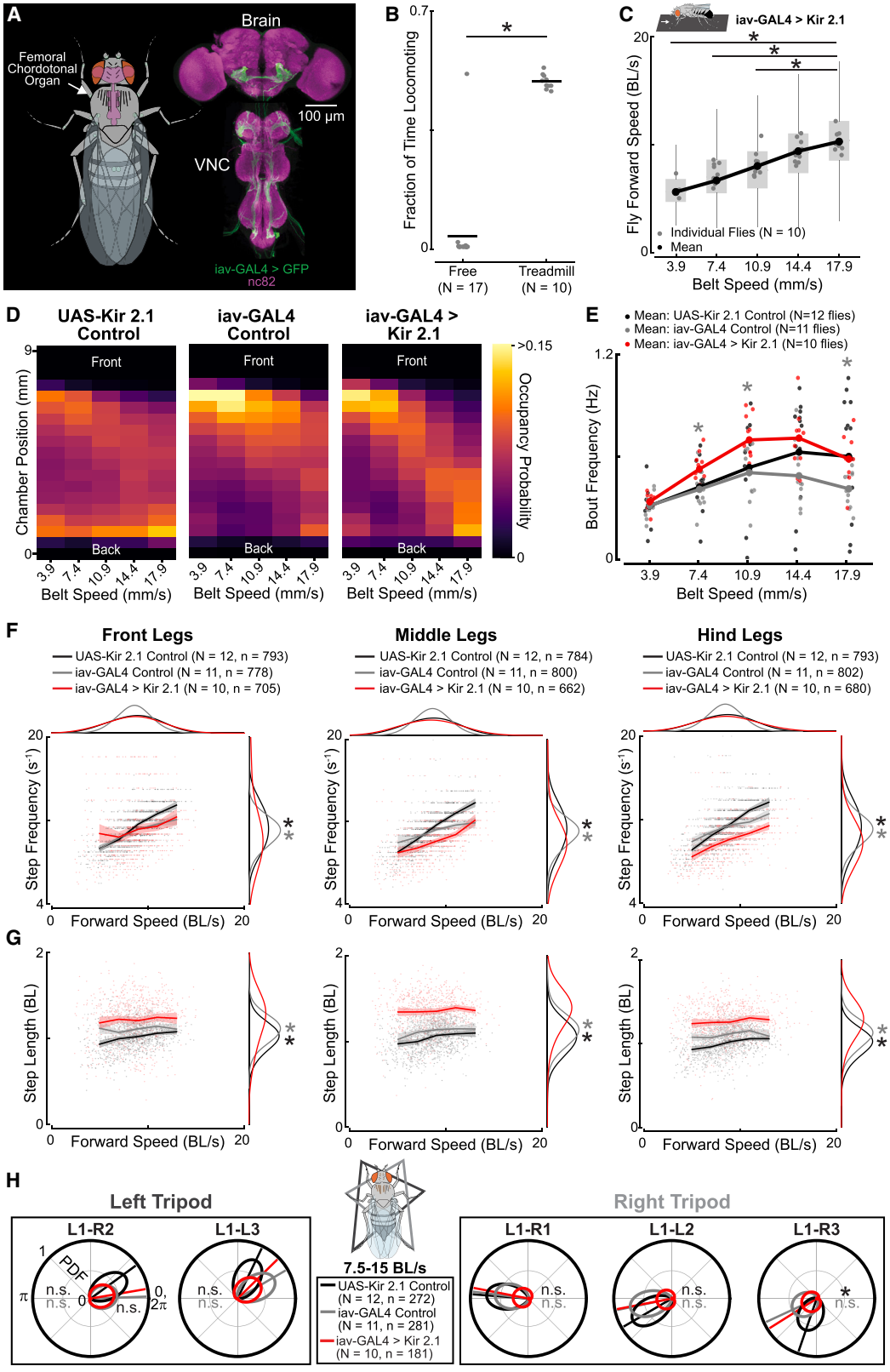

(legend on next page)

Please cite this article in press as: Pratt et al., Miniature linear and split-belt treadmills reveal mechanisms of adaptive motor control in walking *Drosophila*, Current Biology (2024), https://doi.org/10.1016/j.cub.2024.08.006

A split-belt treadmill reveals that middle legs correct for rotational perturbations

We next engineered a split-belt treadmill to investigate behavioral mechanisms of adaptive motor control in walking flies (Figure 5A). We compared the leg kinematics of walking flies while the belts moved at the same speed (tied) versus when the belts moved at different speeds (split: slow and fast), focusing our analysis on periods of forward, straight walking where the left legs were on the left belt and the right legs were on the right belt (STAR Methods; Figure 5B, left; Video S7). We tested splits in both directions and pooled symmetric conditions for subsequent analyses.

We found that flies achieved straight walking by modifying spatial rather than temporal step kinematics. For instance, flies significantly altered where the legs contacted or lifted off of the ground (i.e., the anterior extreme position [AEP] and posterior extreme position [PEP]; Figure 5B, schematic). Specifically, the mean AEP shifted posteriorly and medially for the front leg on the fast belt and laterally for the front leg on the slow belt (Figure 5B, left). The front leg's mean PEP also shifted posteriorly when on the fast belt (Figure 5B, right). The middle leg's AEP shifted medially when on the fast belt but translated posteriorly and laterally on the slow belt (Figure 5B, left). Meanwhile, the PEP of the middle legs shifted in the opposite direction. The hindleg shifted its mean PEP in a similar manner along the longitudinal axis (Figure 5B, right). The changes in leg placement of the middle and hindlegs were also reflected by changes in their stance distance, which describes the distance that each leg moves along the longitudinal and lateral body axes during the stance phase of the step cycle (Figure 5C). Stance duration, the timing component of the stance phase of the step cycle, did not change (Figure 5D), which suggests that changes in spatial leg movement dictate the speed at which legs moved through their step cycle (Figure 5E). For instance, the decrease in stance distance of the middle leg on the slow belt resulted in a slower step speed. Although changes in step speed could in principle have been achieved by altering temporal kinematics, spatial kinematics, or a combination of both, our results suggest that flies overcome the belt asymmetries to maintain forward locomotion by specifically adjusting the step size of the middle legs.

Split-belt walking had weaker effects on inter-leg coordination. For instance, there was a small, though statistically significant, difference in the probability of 3 or 6 legs being in stance during asymmetric belt movement compared with when the belts were tied in speed (Figure 5F). The mean phase offsets between legs were only different for the hindlegs but not for the front or middle legs (Figure 5G). Interestingly, we found that tripod coordination strength[56] (i.e., the strength of the coupling between the legs within a tripod) increased when the ipsilateral front and hindlegs walked on the faster belt during the split condition (Figure 5H). These subtle changes in inter-leg coordination may produce more coupled movement for legs within a tripod, which could help correct for the rotational perturbation induced by the treadmill. In summary, flies use kinematic modifications to the middle legs, in addition to other small kinematic changes, to achieve straight walking during split-belt walking.

DISCUSSION

In this study, we engineered miniature linear and split-belt treadmills for walking *Drosophila* (Figure 1). Flies walking on the treadmill exhibited similar walking behavior, step kinematics, and inter-leg coordination to freely walking flies (Figure 2). The treadmill allowed us to achieve 3D tracking of untethered fly walking, which provided support that flies elevate their body height as they walk faster (Figure 1H). We also used the linear treadmill to show that flies lacking mechanosensory feedback from chordotonal neurons and other proprioceptors are able to walk at higher speeds if compelled to do so (Figure 4). Across

Figure 4. Silencing mechanosensory chordotonal neurons alters step kinematics across walking speeds and has weak effects on inter-leg coordination

(A) A schematic of the locations of chordotonal neurons (green), including the femoral chordotonal organ (white arrow), labeled by the iav-GAL4 driver line. The axons of chordotonal neurons (green) are shown in the max-intensity projection of a confocal stack of the fly brain and VNC (magenta).

(B) Flies with silenced chordotonal neurons (iav-GAL4> Kir 2.1; see table in STAR Methods for full genotype) spent more walking on the treadmill compared with the arena. A t test was used to compare (*$p < 0.05$) the locomotion fractions between iav-GAL4 > Kir 2.1 flies walking in the arena and on the treadmill. Gray dots: individual flies; black lines are means.

(C) The flies in (B) significantly increased their forward walking speed as the belt speed increased (t test; *$p < 0.05$). *N*, number of flies. Boxplots (box, 25th–75th percentile; whiskers, 1.5 IQR from lower and upper quartiles) show the distribution of pooled data. Black line connects the mean forward speed for all flies for each belt speed. Gray dots are the median forward speed of each fly.

(D) Heatmap of the occupancy probability along the chamber for UAS-Kir 2.1 control (see table in STAR Methods for full genotype), iav-GAL4 control, and iav-GAL4 > Kir 2.1 flies.

(E) Bout frequency at each belt speed for UAS-Kir 2.1 control (black), iav-GAL4 control (gray), and iav-GAL4 > Kir 2.1 flies (red). A t test was used to determine statistical significance (*$p < 0.0167$) between flies with chordotonal neurons silenced and each genetically matched control. Big dots: mean across flies at each belt speed. Small dots are the mean bout frequency for each fly. *N*, number of flies.

(F) The step frequency of the front (left), middle (center), and hind (right) legs was lower across walking speeds for flies lacking chordotonal feedback (red) compared with controls (UAS-Kir 2.1 control, black; iav-GAL4 control, gray). Lines are speed-binned averages (2 BL/s bins from 5 to 14 BL/s) for each kinematic parameter, and the 95% confidence interval is shown by the shaded region. The scatter plots of the two genotypes were slightly offset so that each could be visually distinct. Chi-squared test for goodness of fit with a Bonferroni correction was used to statistically compare (*$p < 0.0167$) each leg pair's step frequency between flies with silenced chordotonal neurons and controls. *N*, number of flies; *n*, number of steps.

(G) Step length was greater across walking speeds for flies lacking chordotonal feedback (red) compared with controls (black and gray). A t test with a Bonferroni correction was used to statistically compare (*$p < 0.0167$) the step length between flies with silenced chordotonal neurons and controls.

(H) The relative phase relationships between the left front leg and each other leg over the speed range 7.5–15 BL/s for flies with silenced chordotonal neurons (red) and controls (black and gray). A two-sample Kuiper test with a Bonferroni correction was used to statistically (*$p < 0.003$) compare the distribution of fly means of iav-GAL4 > Kir 2.1 flies to each of the controls. *N*, number of flies. *n*, number of phase comparisons.

See also Figure S2 and Video S6.

Please cite this article in press as: Pratt et al., Miniature linear and split-belt treadmills reveal mechanisms of adaptive motor control in walking *Drosophila*, Current Biology (2024), https://doi.org/10.1016/j.cub.2024.08.006

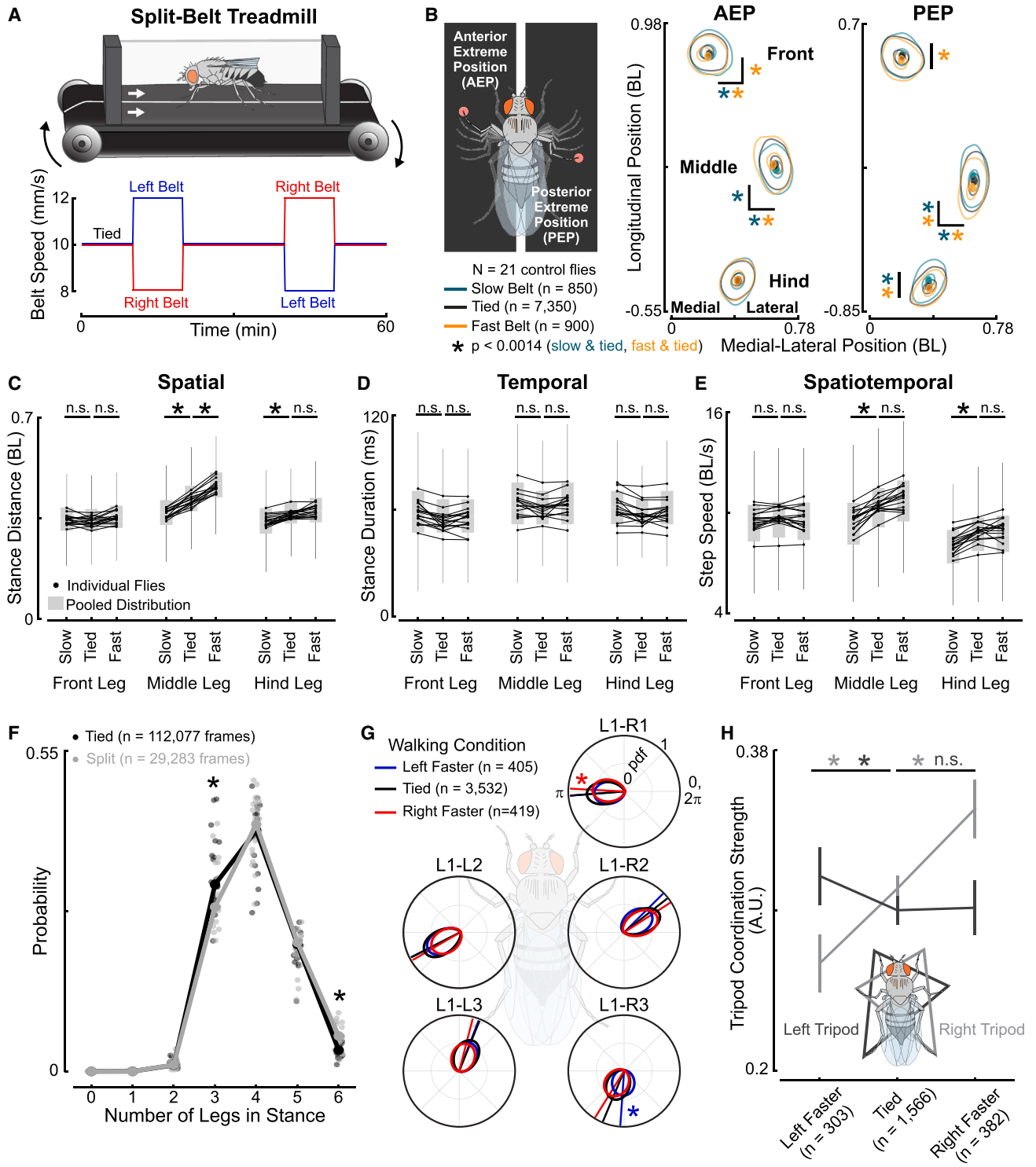

Figure 5. A split-belt treadmill reveals that flies adjust spatial kinematics to correct for rotational perturbations

(A) A schematic of the split-belt treadmill (top) and the belt speed protocol (bottom). The split-belt treadmill consists of two independently controlled belts, which were initially driven at the same speed (tied). The right (red) and left (blue) belts then differed in speed by 40%, and the direction of the speed change reversed on the subsequent split period.

(B) Schematic illustrating that the anterior extreme position (AEP) is where a leg first contacts the ground, and the posterior extreme position (PEP) is where a leg takes off from the ground. AEP and PEP distributions (left and right, respectively) are shown for when legs walked on belts during the tied condition (black) or on the slow (teal) and fast (orange) belt during the split condition. Distributions are shown by kernel density estimations, and means are denoted by dots.

(legend continued on next page)

Please cite this article in press as: Pratt et al., Miniature linear and split-belt treadmills reveal mechanisms of adaptive motor control in walking *Drosophila*, Current Biology (2024), https://doi.org/10.1016/j.cub.2024.08.006

all walking speeds, silencing chordotonal mechanosensory neurons altered the motor control of individual legs and more subtly impacted the coordination between legs. Finally, we found that flies can maintain a forward heading on a split-belt treadmill by adjusting the step size of their middle legs (Figure 5). These insights illustrate how treadmills fill an important gap between freely walking and tethered preparations for investigating neural and behavioral mechanisms of fly locomotion.

Although our primary goal was to compare treadmill and freely walking flies, we also took the opportunity to examine walking kinematics of tethered flies (Figure 2). The advantage of tethered walking is that it enables full 3D joint tracking,[45,46] spatially targeted optogenetic stimulation,[27] and recordings of neural activity with calcium imaging[47] or electrophysiology.[48,49] However, our results suggest that studies of tethered walking should be interpreted with caution because walking kinematics of tethered flies differ in subtle but important ways from untethered flies. Although speed-dependent changes in walking kinematics and coordination were consistent between tethered and untethered flies, the magnitude of step kinematics and the coupling strength between legs were different. One reason for these differences may be that tethered flies walk on a sphere (i.e., a foam ball), whereas treadmill and freely walking flies walk on a flat surface. Tethered flies also do not support their own body weight but instead use their legs to rotate the floating sphere, a configuration that is unlikely to mimic normal ground reaction forces. Indeed, prior work showed that changing the load on the body alters walking kinematics in freely walking flies.[57] On the other hand, it is remarkable that flies and other animals walk at all while tethered on a floating sphere. Given the major mechanical differences between tethered and untethered conditions, the kinematic differences we found are relatively subtle.

One of our motivations for developing a treadmill system for flies was to investigate the role of mechanosensory feedback across walking speeds. Prior work has suggested that proprioception is most important at slower walking speeds and that flies use a more feedforward motor program when walking faster.[8] However, testing this hypothesis has been challenging because silencing mechanosensory neurons causes flies to walk less and at lower velocities.[7] The linear treadmill makes it possible to drive fly locomotion across a wide range of speeds, including after genetic manipulations to mechanosensory neurons. We found that silencing mechanosensory feedback alters step kinematics across all walking speeds (Figures 4F and 4G). Indeed, the greatest deviation in step kinematics between control and experimental flies occurred at faster walking speeds. The lack of mechanosensory feedback had a minimal impact on inter-leg coordination (Figure 4H). We chose to use a blunt manipulation with a broad driver line (iav-Gal4) to illustrate the utility of the treadmill for driving walking even when mechanosensory feedback is profoundly altered. We also used a more specific driver line that labeled a subset of hair plate and campaniform sensilla neurons (Figure S2). Silencing these neurons produced similar kinematic deficits to the chordotonal neuron manipulations. One important caveat is that we expressed Kir 2.1 in sensory neurons throughout development, which may have produced compensation in circuit wiring or function. In the future, it will be interesting to silence mechanosensory feedback of flies walking on the treadmill with more temporal and genetic specificity, for example, using optogenetic manipulation of proprioceptor subtypes in the femoral chordotonal organ.[28,29] Our results are consistent with the hypothesis that proprioceptors contribute primarily to individual leg kinematics, whereas descending commands from the brain[8] or feedback signals from other populations of proprioceptors may have more influence on inter-leg coordination.[63]

In hexapod insects, each pair of legs plays a specialized role in controlling locomotion. In freely walking insects, the front legs are typically used for steering,[30] while the hindlegs contribute to propulsion and jumping.[64–66] Using the split-belt treadmill, we found that the middle legs play a unique role in correcting for perturbations that displace flies from a forward walking trajectory (Figure 5). The middle legs are ideally positioned to stably pivot the body of the fly about its center of mass, like rowing a boat from its center. In larger insects, the middle legs have been shown to play a role in executing tight turns.[67] Although the split-belt treadmill puts the fly in artificial circumstances, it mimics many situations in the wild when flies may need to perform rotational body corrections. For example, heterogeneous terrain, meddlesome conspecifics, or unilateral wind gusts could asymmetrically act on the movement of the left and right legs to induce a rotation of the body. In the future, the split-belt treadmill may also provide a useful method to study the neural mechanisms that underlie adaptive heading

Bootstrapping with a Bonferroni correction was used to statistically (*$p < 0.0014$) compare the means of the tied and split distributions. *N*, number of flies; *n*, number of steps.

(C) Stance distance during slow, tied, and fast belt conditions. Boxplots (box, 25th–75th percentile; whiskers, 1.5 IQR from lower and upper quartiles) show the distribution of pooled data. Black lines connect the mean stance distances (black dots) across belt conditions for each fly. A t test with a Bonferroni correction was used to statistically (*$p < 0.002$) compare the mean stance distances across flies of each split condition to the tied belt condition.

(D) Stance duration did not change across conditions for any leg.

(E) Step speed across belt conditions.

(F) Probability of 0–6 legs being in stance when the belts were tied (black) or split (gray) in speed. A t test determined statistical differences between belt conditions from the means of flies (*$p < 0.05$). Dots connected by lines are the global probabilities. Individual dots are the probability that a given fly shows a certain number of legs in stance.

(G) Polar plots of the relative phase between the left front leg and the other legs when the belts were tied (black) or split (left faster, blue; right faster, red) in speed. A two-sample Kuiper test with a Bonferroni correction was used to statistically (*$p < 0.003$) compare the means of flies in the tied condition to each split condition. Solid lines, average relative phase. *n*, number of phase comparisons.

(H) Tripod coordination strength was significantly greater (t test; *$p < 0.05$) when the ipsilateral front and hindlegs of a tripod were walking on the faster belt compared with the tied condition. Lines (dark gray, left tripod; light gray, right tripod) connect the means across the belt conditions. Error bars represent the 95% confidence intervals. *n*, number of tripod steps.

See also Video S7.

stabilization in walking flies,[68] particularly the postural and heading dynamics that lead to straight walking in the face of lateral perturbations.

In addition to their utility for investigating sensorimotor control of fly walking, we anticipate several additional applications of miniature treadmill systems. One will be to investigate motor adaptation during split-belt walking, a phenomenon that has been extensively studied in mammals.[69] The split-belt treadmill is also used as a clinical tool for diagnosing cerebellar deficits[70] and post-stroke rehabilitation[22] in humans. The linear treadmill may also be useful for the study of insect respiratory physiology, which has previously been studied during flight[71] and in running cockroaches[15] and tarantulas.[72] Finally, because our treadmill system is constructed of simple and inexpensive belts, pulleys, and motors, it can be easily customized to study other walking insects, such as ants[73] and snow flies.[74]

RESOURCE AVAILABILITY

Lead contact

Further information and requests for resources and reagents should be directed to and will be fulfilled by the lead contact, John C. Tuthill (tuthill@uw.edu).

Materials availability

The R93D09 AD: VT061711 DBD split-GAL4 driver line used in this study is available upon request from the lead contact. The source of the wild-type strains and other driver lines used in this study are listed in the key resources table.

Data and code availability

Data is available on Dryad (https://doi.org/10.5061/dryad.mpg4f4r73). Code for analyzing and visualizing treadmill, freely, and tethered walking kinematics is located on GitHub (https://github.com/Prattbuw/Treadmill_Paper). The. stl and.f3d files used for the 3D printed treadmill chamber and Python scripts to acquire high-speed video and control the treadmills are also located there. Any additional requests for information required to reanalyze data associated with this paper or to operate the treadmill systems can be directed to the lead contact.

ACKNOWLEDGMENTS

We thank Max Mauer for engineering the first prototype of the treadmill, Sarah Walling-Bell and Srinidhi Naidu for performing some of the initial treadmill experiments, Eric Martinson for valuable advice and technical support throughout the development of the treadmill systems, Tom Daniel and Jeff Riffell for letting us use their 3D printing equipment and providing advice on the development of the treadmill chamber, Michael Dickinson for designing the fly cartoons many years ago and reminding us of it often, Anne Sustar for the brain and VNC images in Figure 4A, Igor Siwanowicz for creating the graphical abstract, and members of the Tuthill and B.W. Brunton labs for feedback on the manuscript. B.G.P. was supported by an NSF Graduate Research Fellowship (Fellow ID: 2018261272). S.-Y.J.L. was supported by T32 NS 99578-3. Other support was provided by National Institutes of Health grants R01NS102333 and U19NS104655, a Searle Scholar Award, a Klingenstein-Simons Fellowship, a Pew Biomedical Scholar Award, a McKnight Scholar Award, a Sloan Research Fellowship, the New York Stem Cell Foundation, and a UW Innovation Award to J.C.T. J.C.T. is a New York Stem Cell Foundation – Robertson Investigator.

AUTHOR CONTRIBUTIONS

B.G.P. and J.C.T. conceived of the study. B.G.P. engineered the linear and split-belt treadmills. B.G.P. developed high-speed videography acquisition scripts and code to control the treadmill belts. B.G.P. collected and analyzed linear and split-belt treadmill data. S.-Y.J.L. collected and analyzed freely walking data. G.M.C. collected and analyzed tethered walking data. B.G.P. and G.M.C. performed the statistical analyses. B.G.P. and J.C.T. wrote the manuscript with input from other authors.

DECLARATION OF INTERESTS

J.C.T. is a member of *Current Biology*'s advisory board.

STAR★METHODS

Detailed methods are provided in the online version of this paper and include the following:

- KEY RESOURCES TABLE
- EXPERIMENTAL MODEL AND STUDY PARTICIPANT DETAILS
  - *Drosophila melanogaster* genotypes used for experiments
- METHOD DETAILS
  - Linear treadmill and experiments
  - Split-belt treadmill and experiments
  - Freely Walking Experiments
  - Tethered Experiments
  - Confocal Imaging of Mechanosensory Neurons
- QUANTIFICATION AND STATISTICAL ANALYSIS
  - Statistical Tests
  - KL Divergence for Kinematic Similarity
  - Kinematic Classification and Quantification

SUPPLEMENTAL INFORMATION

Supplemental information can be found online at https://doi.org/10.1016/j.cub.2024.08.006.

Received: February 28, 2024
Revised: July 8, 2024
Accepted: August 5, 2024
Published: August 30, 2024

REFERENCES

1. Couzin-Fuchs, E., Kiemel, T., Gal, O., Ayali, A., and Holmes, P. (2015). Intersegmental coupling and recovery from perturbations in freely running cockroaches. J. Exp. Biol. *218*, 285–297. https://doi.org/10.1242/jeb.112805.
2. Eng, J.J., Winter, D.A., and Patla, A.E. (1994). Strategies for recovery from a trip in early and late swing during human walking. Exp. Brain Res. *102*, 339–349. https://doi.org/10.1007/BF00227520.
3. Tuthill, J.C., and Wilson, R.I. (2016). Mechanosensation and adaptive motor control in insects. Curr. Biol. *26*, R1022–R1038. https://doi.org/10.1016/j.cub.2016.06.070.
4. Andersson, O., and Grillner, S. (1983). Peripheral control of the cat's step cycle. II. Entrainment of the central pattern generators for locomotion by sinusoidal hip movements during "fictive locomotion.". Acta Physiol. Scand. *118*, 229–239. https://doi.org/10.1111/j.1748-1716.1983.tb07267.x.
5. Dietz, V. (2002). Proprioception and locomotor disorders. Nat. Rev. Neurosci. *3*, 781–790. https://doi.org/10.1038/nrn939.
6. Chesler, A.T., Szczot, M., Bharucha-Goebel, D., Čeko, M., Donkervoort, S., Laubacher, C., Hayes, L.H., Alter, K., Zampieri, C., Stanley, C., et al. (2016). The role of PIEZO2 in human Mechanosensation. N. Engl. J. Med. *375*, 1355–1364. https://doi.org/10.1056/NEJMoa1602812.
7. Mendes, C.S., Bartos, I., Akay, T., Márka, S., and Mann, R.S. (2013). Quantification of gait parameters in freely walking wild type and sensory deprived Drosophila melanogaster. eLife *2*, e00231. https://doi.org/10.7554/eLife.00231.

8. Bidaye, S.S., Bockemühl, T., and Büschges, A. (2018). Six-legged walking in insects: how CPGs, peripheral feedback, and descending signals generate coordinated and adaptive motor rhythms. J. Neurophysiol. *119*, 459–475. https://doi.org/10.1152/jn.00658.2017.

9. Bélanger, M., Drew, T., Provencher, J., and Rossignol, S. (1996). A comparison of treadmill locomotion in adult cats before and after spinal transection. J. Neurophysiol. *76*, 471–491. https://doi.org/10.1152/jn.1996.76.1.471.

10. Hasan, Z., and Stuart, D.G. (1988). Animal solutions to problems of movement control: the role of proprioceptors. Annu. Rev. Neurosci. *11*, 199–223. https://doi.org/10.1146/annurev.ne.11.030188.001215.

11. Wetzel, M.C., and Stuart, D.G. (1976). Ensemble characteristics of cat locomotion and its neural control. Prog. Neurobiol. *7*, 1–98. https://doi.org/10.1016/0301-0082(76)90002-2.

12. Dean, J., and Wendler, G. (1983). Stick insect locomotion on a walking wheel: interleg coordination of leg position. J. Exp. Biol. *103*, 75–94. https://doi.org/10.1242/jeb.103.1.75.

13. Foth, E., and Bässler, U. (1985). Leg movements of stick insects walking with five legs on a treadwheel and with one leg on a motor-driven belt. I. General results and 1:1-coordination. Biol. Cybern. *51*, 313–318. https://doi.org/10.1007/BF00336918.

14. Foth, E., and Graham, D. (1983). Influence of loading parallel to the body axis on the walking coordination of an insect. Biol. Cybern. *47*, 17–23. https://doi.org/10.1007/BF00340065.

15. Herreid, C.F., and Full, R.J. (1984). Cockroaches on a treadmill: aerobic running. J. Insect Physiol. *30*, 395–403. https://doi.org/10.1016/0022-1910(84)90097-0.

16. Herreid, C.F., II, Full, R.J., and Prawel, D.A. (1981). Energetics of cockroach locomotion. J. Exp. Biol. *94*, 189–202. https://doi.org/10.1242/jeb.94.1.189.

17. Watson, J.T., and Ritzmann, R.E. (1998). Leg kinematics and muscle activity during treadmill running in the cockroach, Blaberus discoidalis: II. Fast running. J. Comp. Physiol. A *182*, 23–33. https://doi.org/10.1007/s003590050154.

18. Whelan, P.J. (1996). Control of locomotion in the decerebrate cat. Prog. Neurobiol. *49*, 481–515. https://doi.org/10.1016/0301-0082(96)00028-7.

19. Fujiki, S., Aoi, S., Funato, T., Sato, Y., Tsuchiya, K., and Yanagihara, D. (2018). Adaptive hindlimb split-belt treadmill walking in rats by controlling basic muscle activation patterns via phase resetting. Sci. Rep. *8*, 17341. https://doi.org/10.1038/s41598-018-35714-8.

20. McVea, D.A., and Pearson, K.G. (2007). Long-lasting, context-dependent modification of stepping in the cat after repeated stumbling-corrective responses. J. Neurophysiol. *97*, 659–669. https://doi.org/10.1152/jn.00921.2006.

21. Kambic, R.E., Roemmich, R.T., and Bastian, A.J. (2023). Joint-level coordination patterns for split-belt walking across different speed ratios. J. Neurophysiol. *129*, 969–983. https://doi.org/10.1152/jn.00323.2021.

22. Reisman, D.S., Wityk, R., Silver, K., and Bastian, A.J. (2007). Locomotor adaptation on a split-belt treadmill can improve walking symmetry post-stroke. Brain *130*, 1861–1872. https://doi.org/10.1093/brain/awm035.

23. Reisman, D.S., Block, H.J., and Bastian, A.J. (2005). Interlimb coordination during locomotion: what can be adapted and stored? J. Neurophysiol. *94*, 2403–2415. https://doi.org/10.1152/jn.00089.2005.

24. Darmohray, D.M., Jacobs, J.R., Marques, H.G., and Carey, M.R. (2019). Spatial and temporal locomotor learning in mouse cerebellum. Neuron *102*, 217–231.e4. https://doi.org/10.1016/j.neuron.2019.01.038.

25. Torres-Oviedo, G., Vasudevan, E., Malone, L., and Bastian, A.J. (2011). Chapter 4. Locomotor adaptation. In Progress in Brain Research, A.M. Green, C.E. Chapman, J.F. Kalaska, and F. Lepore, eds. (Elsevier), pp. 65–74. https://doi.org/10.1016/B978-0-444-53752-2.00013-8.

26. Clarac, F. (1984). Spatial and temporal co-ordination during walking in crustacea. Trends Neurosci. *7*, 293–298. https://doi.org/10.1016/S0166-2236(84)80199-X.

27. Agrawal, S., Dickinson, E.S., Sustar, A., Gurung, P., Shepherd, D., Truman, J.W., and Tuthill, J.C. (2020). Central processing of leg proprioception in Drosophila. eLife *9*, e60299. https://doi.org/10.7554/eLife.60299.

28. Chen, C., Agrawal, S., Mark, B., Mamiya, A., Sustar, A., Phelps, J.S., Lee, W.A., Dickson, B.J., Card, G.M., and Tuthill, J.C. (2021). Functional architecture of neural circuits for leg proprioception in Drosophila. Curr. Biol. *31*, 5163–5175.e7. https://doi.org/10.1016/j.cub.2021.09.035.

29. Chockley, A.S., Dinges, G.F., Di Cristina, G., Ratican, S., Bockemühl, T., and Büschges, A. (2022). Subsets of leg proprioceptors influence leg kinematics but not interleg coordination in Drosophila melanogaster walking. J. Exp. Biol. *225*, jeb244245. https://doi.org/10.1242/jeb.244245.

30. Isakov, A., Buchanan, S.M., Sullivan, B., Ramachandran, A., Chapman, J.K.S., Lu, E.S., Mahadevan, L., and de Bivort, B. (2016). Recovery of locomotion after injury in *Drosophila* depends on proprioception. J. Exp. Biol. Jeb, 133652. https://doi.org/10.1242/jeb.133652.

31. Mamiya, A., Sustar, A., Siwanowicz, I., Qi, Y., Lu, T.-C., Gurung, P., Chen, C., Phelps, J.S., Kuan, A.T., Pacureanu, A., et al. (2023). Biomechanical origins of proprioceptor feature selectivity and topographic maps in the Drosophila leg. Neuron *111*, 3230–3243.e14. https://doi.org/10.1016/j.neuron.2023.07.009.

32. Mamiya, A., Gurung, P., and Tuthill, J.C. (2018). Neural coding of leg proprioception in Drosophila. Neuron *100*, 636–650.e6. https://doi.org/10.1016/j.neuron.2018.09.009.

33. Dorkenwald, S., Matsliah, A., Sterling, A.R., Schlegel, P., Yu, S.C., McKellar, C.E., Lin, A., Costa, M., Eichler, K., Yin, Y., et al. (2023). Neuronal wiring diagram of an adult brain. Preprint at bioRxiv. https://doi.org/10.1101/2023.06.27.546656.

34. Azevedo, A., Lesser, E., Phelps, J.S., Mark, B., Elabbady, L., Kuroda, S., Sustar, A., Moussa, A., Khandelwal, A., Dallmann, C.J., et al. (2024). Connectomic reconstruction of a female Drosophila ventral nerve cord. Nature *631*, 360–368. https://doi.org/10.1038/s41586-024-07389-x.

35. Takemura, S., Hayworth, K.J., Huang, G.B., Januszewski, M., Lu, Z., Marin, E.C., Preibisch, S., Xu, C.S., Bogovic, J., Champion, A.S., et al. (2024). A connectome of the male Drosophila ventral nerve cord. Preprint at eLife. https://doi.org/10.7554/eLife.97769.1.

36. Berendes, V., Zill, S.N., Büschges, A., and Bockemühl, T. (2016). Speed-dependent interplay between local pattern-generating activity and sensory signals during walking in Drosophila. J. Exp. Biol. *219*, 3781–3793. https://doi.org/10.1242/jeb.146720.

37. Buchner, E. (1976). Elementary movement detectors in an insect visual system. Biol. Cybern. *24*, 85–101. https://doi.org/10.1007/BF00360648.

38. Creamer, M.S., Mano, O., and Clark, D.A. (2018). Visual control of walking speed in Drosophila. Neuron *100*, 1460–1473.e6. https://doi.org/10.1016/j.neuron.2018.10.028.

39. Götz, K.G., and Wenking, H. (1973). Visual control of locomotion in the walking fruit fly Drosophila. J. Comp. Physiol. *85*, 235–266. https://doi.org/10.1007/BF00694232.

40. DeAngelis, B.D., Zavatone-Veth, J.A., and Clark, D.A. (2019). The manifold structure of limb coordination in walking Drosophila. eLife *8*, e46409. https://doi.org/10.7554/eLife.46409.

41. Fujiwara, T., Brotas, M., and Chiappe, M.E. (2022). Walking strides direct rapid and flexible recruitment of visual circuits for course control in Drosophila. Neuron *110*, 2124–2138.e8. https://doi.org/10.1016/j.neuron.2022.04.008.

42. Simon, J.C., and Dickinson, M.H. (2010). A new chamber for studying the behavior of Drosophila. PLoS One *5*, e8793. https://doi.org/10.1371/journal.pone.0008793.

43. Strauss, R., and Heisenberg, M. (1990). Coordination of legs during straight walking and turning in Drosophila melanogaster. J. Comp. Physiol. A *167*, 403–412. https://doi.org/10.1007/BF00192575.

44. York, R.A., Brezovec, L.E., Coughlan, J., Herbst, S., Krieger, A., Lee, S.-Y., Pratt, B., Smart, A.D., Song, E., Suvorov, A., et al. (2022). The evolutionary

trajectory of drosophilid walking. Curr. Biol. *32*, 3005–3015.e6. https://doi.org/10.1016/j.cub.2022.05.039.

45. Günel, S., Rhodin, H., Morales, D., Campagnolo, J., Ramdya, P., and Fua, P. (2019). DeepFly3D, a deep learning-based approach for 3D limb and appendage tracking in tethered, adult Drosophila. eLife *8*, e48571. https://doi.org/10.7554/eLife.48571.
46. Karashchuk, P., Rupp, K.L., Dickinson, E.S., Walling-Bell, S., Sanders, E., Azim, E., Brunton, B.W., and Tuthill, J.C. (2021). Anipose: A toolkit for robust markerless 3D pose estimation. Cell Rep. *36*, 109730. https://doi.org/10.1016/j.celrep.2021.109730.
47. Seelig, J.D., Chiappe, M.E., Lott, G.K., Dutta, A., Osborne, J.E., Reiser, M.B., and Jayaraman, V. (2010). Two-photon calcium imaging from head-fixed Drosophila during optomotor walking behavior. Nat. Methods *7*, 535–540. https://doi.org/10.1038/nmeth.1468.
48. Fujiwara, T., Cruz, T.L., Bohnslav, J.P., and Chiappe, M.E. (2017). A faithful internal representation of walking movements in the Drosophila visual system. Nat. Neurosci. *20*, 72–81. https://doi.org/10.1038/nn.4435.
49. Turner-Evans, D., Wegener, S., Rouault, H., Franconville, R., Wolff, T., Seelig, J.D., Druckmann, S., and Jayaraman, V. (2017). Angular velocity integration in a fly heading circuit. eLife *6*, e23496. https://doi.org/10.7554/eLife.23496.
50. Mathis, A., Mamidanna, P., Cury, K.M., Abe, T., Murthy, V.N., Mathis, M.W., and Bethge, M. (2018). DeepLabCut: markerless pose estimation of user-defined body parts with deep learning. Nat. Neurosci. *21*, 1281–1289. https://doi.org/10.1038/s41593-018-0209-y.
51. Sorribes, A., Armendariz, B.G., Lopez-Pigozzi, D., Murga, C., and de Polavieja, G.G. (2011). The origin of behavioral bursts in decision-making circuitry. PLoS Comp. Biol. *7*, e1002075. https://doi.org/10.1371/journal.pcbi.1002075.
52. Chun, C., Biswas, T., and Bhandawat, V. (2021). Drosophila uses a tripod gait across all walking speeds, and the geometry of the tripod is important for speed control. eLife *10*, e65878. https://doi.org/10.7554/eLife.65878.
53. Full, R.J., and Tu, M.S. (1991). Mechanics of a rapid running insect: two-, four-and six-legged locomotion. J. Exp. Biol. *156*, 215–231. https://doi.org/10.1242/jeb.156.1.215.
54. Struzik, A., Karamanidis, K., Lorimer, A., Keogh, J.W.L., and Gajewski, J. (2021). Application of leg, vertical, and joint stiffness in running performance: a literature overview. Appl. Bionics Biomech. *2021*, 9914278. https://doi.org/10.1155/2021/9914278.
55. Szczecinski, N.S., Bockemühl, T., Chockley, A.S., and Büschges, A. (2018). Static stability predicts the continuum of interleg coordination patterns in Drosophila. J. Exp. Biol. *221*, jeb189142. https://doi.org/10.1242/jeb.189142.
56. Wosnitza, A., Bockemühl, T., Dübbert, M., Scholz, H., and Büschges, A. (2013). Inter-leg coordination in the control of walking speed in Drosophila. J. Exp. Biol. *216*, 480–491. https://doi.org/10.1242/jeb.078139.
57. Mendes, C.S., Rajendren, S.V., Bartos, I., Márka, S., and Mann, R.S. (2014). Kinematic responses to changes in walking orientation and gravitational load in Drosophila melanogaster. PLoS One *9*, e109204. https://doi.org/10.1371/journal.pone.0109204.
58. Azevedo, A.W., Dickinson, E.S., Gurung, P., Venkatasubramanian, L., Mann, R.S., and Tuthill, J.C. (2020). A size principle for recruitment of Drosophila leg motor neurons. eLife *9*, e56754. https://doi.org/10.7554/eLife.56754.
59. Pereira, T.D., Aldarondo, D.E., Willmore, L., Kislin, M., Wang, S.S.-H., Murthy, M., and Shaevitz, J.W. (2019). Fast animal pose estimation using deep neural networks. Nat. Methods *16*, 117–125. https://doi.org/10.1038/s41592-018-0234-5.
60. Cruse, H. (1990). What mechanisms coordinate leg movement in walking arthropods? Trends Neurosci. *13*, 15–21. https://doi.org/10.1016/0166-2236(90)90057-H.
61. Cruse, H. (1985). Which parameters control the leg movement of a walking insect?: II. The start of the swing phase. J. Exp. Biol. *116*, 357–362. https://doi.org/10.1242/jeb.116.1.357.
62. Card, G., and Dickinson, M. (2008). Performance trade-offs in the flight initiation of Drosophila. J. Exp. Biol. *211*, 341–353. https://doi.org/10.1242/jeb.012682.
63. Tuthill, J.C., and Azim, E. (2018). Proprioception. Curr. Biol. *28*, R194–R203. https://doi.org/10.1016/j.cub.2018.01.064.
64. Burrows, M. (2013). Jumping mechanisms of treehopper insects (Hemiptera, Auchenorrhyncha, Membracidae). J. Exp. Biol. *216*, 788–799. https://doi.org/10.1242/jeb.078741.
65. Burrows, M. (2007). Anatomy of the hind legs and actions of their muscles during jumping in leafhopper insects. J. Exp. Biol. *210*, 3590–3600. https://doi.org/10.1242/jeb.009100.
66. Card, G., and Dickinson, M.H. (2008). Visually mediated motor planning in the escape response of Drosophila. Curr. Biol. *18*, 1300–1307. https://doi.org/10.1016/j.cub.2008.07.094.
67. Cruse, H., Ehmanns, I., Stübner, S., and Schmitz, J. (2009). Tight turns in stick insects. J. Comp. Physiol. A Neuroethol. Sens. Neural Behav. Physiol. *195*, 299–309. https://doi.org/10.1007/s00359-008-0406-3.
68. Haberkern, H., Chitnis, S.S., Hubbard, P.M., Goulet, T., Hermundstad, A.M., and Jayaraman, V. (2022). Maintaining a stable head direction representation in naturalistic visual environments. Preprint at bioRxiv. https://doi.org/10.1101/2022.05.17.492284.
69. Hinton, D.C., Conradsson, D.M., and Paquette, C. (2020). Understanding human neural control of short-term gait adaptation to the split-belt treadmill. Neuroscience *451*, 36–50. https://doi.org/10.1016/j.neuroscience.2020.09.055.
70. Hoogkamer, W., Bruijn, S.M., Sunaert, S., Swinnen, S.P., Van Calenbergh, F., and Duysens, J. (2015). Adaptation and aftereffects of split-belt walking in cerebellar lesion patients. J. Neurophysiol. *114*, 1693–1704. https://doi.org/10.1152/jn.00936.2014.
71. Lehmann, F.-O. (2001). Matching spiracle opening to metabolic need during flight in Drosophila. Science *294*, 1926–1929. https://doi.org/10.1126/science.1064821.
72. Shillington, C., and Peterson, C.C. (2002). Energy metabolism of male and female tarantulas (Aphonopelma anax) during locomotion. J. Exp. Biol. *205*, 2909–2914. https://doi.org/10.1242/jeb.205.18.2909.
73. Dahmen, H., Wahl, V.L., Pfeffer, S.E., Mallot, H.A., and Wittlinger, M. (2017). Naturalistic path integration of Cataglyphis desert ants on an air-cushioned lightweight spherical treadmill. J. Exp. Biol. *220*, 634–644. https://doi.org/10.1242/jeb.148213.
74. Golding, D., Rupp, K.L., Sustar, A., Pratt, B., and Tuthill, J.C. (2023). Snow flies self-amputate freezing limbs to sustain behavior at sub-zero temperatures. Curr. Biol. *33*, 4549–4556.e3. https://doi.org/10.1016/j.cub.2023.09.002.
75. Pereira, T.D., Tabris, N., Matsliah, A., Turner, D.M., Li, J., Ravindranath, S., Papadoyannis, E.S., Normand, E., Deutsch, D.S., Wang, Z.Y., et al. (2022). SLEAP: A deep learning system for multi-animal pose tracking. Nat. Methods *19*, 486–495. https://doi.org/10.1038/s41592-022-01426-1.
76. Moore, R.J.D., Taylor, G.J., Paulk, A.C., Pearson, T., van Swinderen, B., and Srinivasan, M.V. (2014). FicTrac: A visual method for tracking spherical motion and generating fictive animal paths. J. Neurosci. Methods *225*, 106–119. https://doi.org/10.1016/j.jneumeth.2014.01.010.
77. Schindelin, J., Arganda-Carreras, I., Frise, E., Kaynig, V., Longair, M., Pietzsch, T., Preibisch, S., Rueden, C., Saalfeld, S., Schmid, B., et al. (2012). Fiji: an open-source platform for biological-image analysis. Nat. Methods *9*, 676–682. https://doi.org/10.1038/nmeth.2019.
78. Seeds, A.M., Ravbar, P., Chung, P., Hampel, S., Midgley, F.M., Mensh, B.D., and Simpson, J.H. (2014). A suppression hierarchy among competing motor programs drives sequential grooming in Drosophila. eLife *3*, e02951. https://doi.org/10.7554/eLife.02951.

Please cite this article in press as: Pratt et al., Miniature linear and split-belt treadmills reveal mechanisms of adaptive motor control in walking *Drosophila*, Current Biology (2024), https://doi.org/10.1016/j.cub.2024.08.006

CellPress

STAR★METHODS

KEY RESOURCES TABLE

REAGENT or RESOURCE	SOURCE	IDENTIFIER
Antibodies		
Goat anti-mouse secondary antibody, Alexa Fluor 633 conjugate	Invitrogen	RRID: AB_141431
Goat anti-rat secondary antibody, Alexa Fluor 488 conjugate	Thermo Fisher Scientific	RRID: AB_2534074
Rat anti-CD8 monoclonal antibody	Thermo Fisher Scientific	RRID: AB_10392843
Mouse anti-Bruchpilot monoclonal antibody	Developmental Studies Hybridoma Ban	RRID: AB_2314866
Deposited data		
Raw and analyzed freely, tethered, and treadmill walking datasets. Treadmill chamber 3D design files.	This Paper	https://doi.org/10.5061/dryad.mpg4f4r73
Experimental models: Organisms/strains		
Wild Type Berlin	Gift from Heisenberg lab, University of Würzburg	N/A
w[*]; P{w[+mC]=iav-GAL4.K}3	Bloomington	RRID: BDSC_52273
w[1118]; P{y[+t7.7]w[+mC]=R93D09-p65.AD}attP40	Bloomington	RRID: BDSC_68586
w[1118]; {{y[+t7.7]w[+mC]=VT061711-GAL4.DBD}attP2	Bloomington	RRID: BDSC_73753
w[1118]; P{y[+t7.7]w[+mC]=R48A07-p65.AD}attP40	Bloomington	RRID: BDSC_71070
w[1118]; P{y[+t7.7]w[+mC]=R39B11-p65.AD}attP40	Bloomington	RRID: BDSC_71040
w[1118]; {{y[+t7.7]w[+mC]=R52A01-GAL4.DBD}attP2	Bloomington	RRID: BDSC_69141
w[1118]	Bloomington	RRID: BDSC_3605
Wild Type DL (Dickinson Lab)	Gift from Dickinson Lab, Caltech	N/A
+ DL; + DL; pJFRC49-10XUAS-IVS-eGFP::Kir2.1(attP2)	Gift from Dickinson Lab, Caltech	N/A
yw, hs flp,UAS-mCD8-GFP; UAS-stingerRed/Cyo; +	Gift from Parrish Lab, University of Washinton	N/A
w[*]; +; P{pJFRC7-020xUAS-IVS-mCD8::GFP}attP2	Gift from Rubin Lab, hhmi, Janelia	N/A
Software and algorithms		
Anipose	Karashchuk et al.[46]	https://anipose.readthedocs.io/en/latest/installation.html
DeepLabCut	Mathis et al.[50]	https://github.com/DeepLabCut/DeepLabCut
SLEAP	Pereira et al.[75]	https://sleap.ai/develop/installation.html
FicTrac	Moore et al.[76]	https://github.com/rjdmoore/fictrac
FIJI	Schindelin et al.[77]	https://imagej.net/software/fiji/
Autodesk Fusion 360	Autodesk	https://www.autodesk.com/products
Treadmill, Analysis, and Visualization Code	This Paper	https://github.com/Prattbuw/Treadmill_Paper

EXPERIMENTAL MODEL AND STUDY PARTICIPANT DETAILS

Adult male *Drosophila melanogaster* between 2-7 days post-eclosion were used for all behavior experiments (see table below). Flies were reared in a 25°C incubator with 14:10 light:dark cycle in vials filled with a standard cornmeal and molasses medium.

Please cite this article in press as: Pratt et al., Miniature linear and split-belt treadmills reveal mechanisms of adaptive motor control in walking *Drosophila*, Current Biology (2024), https://doi.org/10.1016/j.cub.2024.08.006

Drosophila melanogaster genotypes used for experiments

Stock Name	Genotype	Figure(s)	Stock Source
WT Berlin	+; +; +	Figures 1, 2, 3, and S1	Gifted from Heisenberg Lab
R52A01 DBD > Kir 2.1 (Control)	w[1118]/+ DL; +/+ DL; pJFRC49-10XUAS-IVS-eGFP::Kir2.1(attP2)/P{y[+t7.7]w[+mC]=R52A01-GAL4.DBD}attP2	Figure S2	Crossed Dickinson Lab Stock U-111 with Bloomington Stock #69141
R93D09 AD: VT061711 DBD > Kir 2.1	w[1118]/+ DL; P{y[+t7.7]w[+mC]=R93D09-p65.AD}attP40/+ DL; P{y[+t7.7]w[+mC]=VT061711-GAL4.DBD}attP2/ pJFRC49-10XUAS-IVS-eGFP::Kir2.1(attP2)	Figure S2	Split-GAL4 made from #68586 and #73753 of Bloomington Drosophila Stock Center crossed with Dickinson Lab Stock U-111
UAS-Kir 2.1 (Control)	w[1118]/ + DL; + / + DL; +/ pJFRC49-10XUAS-IVS-eGFP::Kir2.1(attP2)	Figure 4	Crossed Dickinson Lab Stock U-111 with Bloomington Stock #3605
iav-GAL4 (Control)	w[*]/+ DL; +/ + DL; P{w[+mC]=iav-GAL4.K}3/ + DL	Figure 4	Crossed Bloomington stock #52273 with Dickinson Lab Stock #W-03
iav-GAL4 > Kir 2.1	w[*]/+ DL; +/+ DL; pJFRC49-10XUAS-IVS-eGFP::Kir2.1(attP2)/P{w[+mC]=iav-GAL4.K}3	Figure 4	Crossed Dickinson Lab Stock U-111 with Bloomington Stock #52273
R48A07 AD > Kir 2.1 (Control)	w[1118]/+ DL; P{+t[7.7]w[=mC]=R48A07-p65.AD}attP40/+ DL; pJFRC49-10XUAS-IVS-eGFP::Kir2.1(attP2)/+	Figure 5	Crossed Dickinson Lab Stock U-111 with Bloomington Stock #71070
R39B11 AD > Kir 2.1 (Control)	w[1118]/+ DL; P{+t[7.7]w[=mC]=R39B11-p65.AD}attP40/+ DL; pJFRC49-10XUAS-IVS-eGFP::Kir2.1(attP2)/+	Figure 5	Crossed Dickinson Lab Stock U-111 with Bloomington Stock #71040

METHOD DETAILS

Linear treadmill and experiments

The key components of the linear treadmill system are a custom 3D-printed chamber (Figure S3A), pulleys, a belt, a DC motor controlled programmatically with a PID controller, and 5 high-speed cameras (Figure S3B). The chamber was designed using 3D CAD software (Autodesk Fusion 360: *Treadmill_Chamber.stl* and *Treadmill_Chamber.f3d* in GitHub repository) and printed with black resin using a high spatial resolution 3D printer (Formlabs Form 2; black resin RS-F2-GPBK-04). The region of the chamber where the fly walked had transparent, sloped walls, a measured length, max width, and height of 8.929 mm (prescribed length was 9.5 mm), 8 mm, and 1.5 mm, respectively. Coverslips that were 22m x 22m and size #1 were used as the transparent walls of the chamber (Electron Microscopy Sciences: #72200-10). Rain-X was applied to the inner surface of the coverslips to limit flies from walking on the glass. The pulleys (B & B Manufacturing: 28MP025M6FA6) were attached to steel bars which rotated with bearings (AST Bearings: SMF126ZZ) that were mounted on custom fabricated brackets. The distance between the brackets was adjustable, which enabled the belt (B & B Manufacturing: 100MXL025UK) held between the pullies to be manually tensioned (e.g. setting brackets further apart resulted in a more tensioned, taut belt). A mounted DC motor (Phidgets: 12V/0.8Kg-cm/46RPM 50:1 DC Gear Motor w/ Encoder ID: 3256E_0) actuated the belt. An infrared ring-light (Olympus Controls: R130-850) was used to illuminate flies on the belt. 5 high-speed cameras (Machine Vision Store; USB 3.0 Basler camera acA800 x 600, Basler AG) with adjustable lenses (Computar: MLM3X-MP) and IR filters (Olympus Controls: FS03-BP850-34) recorded flies walking on the belt and within the chamber at 180 fps. The DC motor and high-speed cameras were controlled using a microcontroller (Phidgets: PhidgetMotorControl 1-Motor ID: 1065_1B) and DAQ (National Instruments: BNC-2110), respectively, and a custom Python script (*linear_treadmill_belt_stim_videography.py* in GitHub repository).

Male *Drosophila* (see table above) were driven to walk on the linear treadmill while the belt's steady state speed was either 3.9, 7.4, 10.9, 14.4, or 17.9 mm/s. To smoothly reach steady-state belt speeds above 3.9mm/s, the belt linearly increased in speed at a rate of

Please cite this article in press as: Pratt et al., Miniature linear and split-belt treadmills reveal mechanisms of adaptive motor control in walking *Drosophila*, Current Biology (2024), https://doi.org/10.1016/j.cub.2024.08.006

3.5 mm/s^2. Wild-type Berlin and iav-GAL4 > Kir 2.1 flies were subjected to each belt speed 10 times, whereas R52A01 DBD > Kir 2.1, iav-GAL4 control, and UAS-Kir 2.1 control flies were presented each belt speed 15 times. Trials in which flies walked at a given belt speed were 10 seconds. There was a 5 second period between trials where the belt moved at 3.9 mm/s and the high-speed videos were saved. DeepLabCut and Anipose[46,50] were used to track the fly's leg tips (i.e. tarsi), head, thorax, abdomen, and key points on the chamber in 3D using 2,250 annotated frames as the training dataset. The test prediction error of the tracking was 5.45 pixels and the reprojection error was 2.88 pixels. Walking kinematics were analyzed and visualized using custom Python scripts (*linear_treadmill_walking_analysis.ipynb* & *linear_treadmill_visualization_walking_comparisons.ipynb* in GitHub repository).

We also tried driving tethered flies to walk on the linear treadmill. Occasionally, the front legs moved with the belt, but the overall movement between legs was uncoordinated. We typically observed legs being dragged along the surface of the belt. It should be noted that we tried many different tether designs, from rigid ones to light-weight, low-resistance ones inspired from a treadmill used for desert ants.[73] Overall, we were unable to drive coordinated walking in tethered flies using the treadmill.

We used several different fly lines as controls for different experiments throughout the paper (see table above). For the experiments in which the neurons labeled by R93D09 AD: VT061711 DBD (HP+CS-GAL4) were silenced (Figure S2), we used R52A01 DBD > Kir 2.1 as a control because the lack of the complete GAL4 construct results in no expression of Kir 2.1. The alternative, Empty-GAL4, is not a sufficient control because it has been previously shown to have expression in the VNC.[78] We found comparable walking kinematics between wild-type flies and split-GAL4 half flies, such as R52A01 DBD > Kir 2.1, R48A07 AD > Kir 2.1, and R39B11 AD > Kir 2.1. Therefore, split-GAL4 half > Kir 2.1 flies were suitable controls. Note that we used split-GAL4 half flies in Figure 5 because these flies serve as controls for future experimental work.

Split-belt treadmill and experiments

The construction of the split-belt chamber was similar to the linear treadmill (Figure S3C). The key difference was the addition of a second independently actuated belt. Therefore, we used smaller belts (B & B Manufacturing: 100MXL012UK) and pulleys (B & B Manufacturing: 28MP012M6FA6), while the chamber size remained the same. We also used DC motors (Phidgets: 12V/3.0Kg-cm/78RPM 51:1 DC Gear Motor w/ Encoder ID: 3263E_1) that were of a newer model. Finally, the frame rate of the high-speed cameras was increased to 200 fps. A custom Python script controlled the motors and cameras (*splitbelt_treadmill_belt_stim_videography.py* in GitHub repository).

Only male flies were used in split-belt experiments (see table above). Flies initially walked on belts that were tied in speed (i.e. 10 mm/s) for 10 minutes. Then, one belt increased in speed by 20% (i.e. 12 mm/s) while the other belt decreased in speed by 20% (i.e. 8 mm/s). This split period also lasted 10 minutes. Following the split period, the belts again moved at 10 mm/s for 10 minutes. At the end of the 10 minutes, this trial structure was repeated, but the belts switched which increased or decreased in speed during the split period. 5 high-speed cameras recorded the movement of the fly during this task and the same key points in the linear treadmill experiments were tracked and reconstructed in 3D. The training dataset consisted of 4,140 annotated frames and the DeepLabCut network achieved a test error of 6.13 pixels. The reprojection error was 1.82 pixels. Custom Python scripts were used to analyze and visualize walking kinematics (*splitbelt_walking_analysis.ipynb* and *splitbelt_walking_visualization.ipynb* in GitHub repository).

Freely Walking Experiments

Groups of 10, 2-7 day old, male wild-type Berlin flies were placed in a 10 cm circular arena with sloped walls (i.e. fly bowl) and allowed to freely walk.[42] A high-speed camera (Machine Vision Store: USB 3.0 Basler camera acA1300-200um, Basler AG) recorded a 2.4 cm x 2.7 cm region of the arena, which had subtle slope of 11 degrees, from above at 150 fps in 10s bouts. Leg tips, head, thorax, and abdomen of flies were tracked using SLEAP, which is optimized for multi-animal pose estimation.[75] Custom Python scripts quantified and visualized walking kinematics (*freely_walking_analysis_visualization.ipynb* in GitHub repository).

Tethered Experiments

De-winged male wild-type Berlin flies, 2-5 days old, were attached to a thin tungsten tether (0.1 mm) with UV curing glue (KOA 300). Flies were then positioned with a micromanipulator on a spherical foam ball (weight: 0.13 g; diameter: 9.08 mm) suspended by a regulated air supply. The 2D trajectory, and forward, rotational, and side-slip velocities of the fly were measured from the movement of the ball with FicTrac.[76] 6 high-speed cameras (Machine Vision Store: USB 3.0 Basler camera acA800 x 600, Basler AG) recorded flies walking on the ball at 300 fps over 2 second bouts. Custom python and MATLAB scripts were used to acquire the high-speed videos. The leg joints, tips, head, and abdomen were tracked and reconstructed in 3D using DeepLabCut and Anipose, respectively. Walking kinematics were analyzed and visualized using Python (*tethered_walking_analysis_visualization.ipynb* in GitHub repository).

Confocal Imaging of Mechanosensory Neurons

We examined the peripheral expression of mechanosensory neurons (Figure S2) to determine which and how many neurons were labeled across the leg pairs by the R93D09 AD: VT061711 DBD split-GAL4 driver line. We drove the expression of mCD8GFP and RedStinger in the neurons labeled by this split-GAL4 line and fixed legs in a 4% formaldehyde (PFA) PBS solution for 20 minutes and then washed three times in a 0.2% Triton X-100 PBS solution. Using an Olympus FV1000 confocal microscope, we imaged the expression of mechanosensory neurons in the legs. We used FIJI[77] to visually inspect the confocal stacks and determine the number and identity of the cells labeled by the split-GAL4 driver line.

Please cite this article in press as: Pratt et al., Miniature linear and split-belt treadmills reveal mechanisms of adaptive motor control in walking *Drosophila*, Current Biology (2024), https://doi.org/10.1016/j.cub.2024.08.006

We additionally used confocal imaging to determine the expression of the above split-GAL4 driver lines (Figure S2) and iav-GAL4 (Figure 4) in brain and VNC. We used the same solution and protocol as above to fix brains and VNC of flies that expressed mCD8::GFP (i.e. pJFRC7-20XUAS-IVS-mCD8::GFP). The fixed brains and VNCs were then put into a blocking solution (5% goat serum, PBS, 0.2% Triton-X) for 20 minutes, followed by being incubated in a blocking and primary antibody solution (1:50 concentration of anti-GFP chicken antibody, 1:50 concentration of anti-brp mouse) for 24 hours at room temperature. They were then washed three times in PBS with 0.2% Triton-X and incubated in a blocking and secondary antibody solution (1:250 concentration of anti-chicken-Alexa 488, 1:250 concentration of anti-mouse-Alexa 633). After this, they were washed three times with PBST and mounted on a slide in Vectashield (Vector Laboratories). The brains and VNCs were imaged using the Olympus FV1000 confocal microscope and image stacks were analyzed in FIJI.[77]

QUANTIFICATION AND STATISTICAL ANALYSIS

Statistical Tests

Chi-squared test and t-tests were used to test for statistical differences in step kinematics and inter-leg coordination between the different walking setups (Figures 1, 2, and 3), control and mechanosensory deficient flies (Figures 4 and S2), and flies walking during split and tied belt conditions (Figure 5). Statistics on step kinematics across the walking setups were conducted on kinematic distributions containing data from all leg pairs and that were associated with a walking speed between 6.5-10.1 BL/s (Figure 2), as well as over narrower speed ranges (Figure S1). The 6.5-10.1 BL/s walking speed range was chosen because it contained 50% of the data across setups given their overlapping speed ranges, ensuring that the kinematic differences we observed weren't due to tethered flies walking slower. The chi-squared test determined whether the proportion of values of a given discretely measured step metric (i.e. step frequency, stance duration, and swing duration) was the same between freely walking flies and those in the other two setups. Additionally, we performed a chi-squared test to statistically compare the step frequency between control and mechanosensory deficient flies (Figures 4 and S2). A Bonferroni correction of 18 was added to account for multiple comparisons (6 legs and 3 setups). Therefore, a significant difference was determined to be $p < 0.0028$. Note that to make the statistical comparisons of step frequency, stance duration, and swing duration between all three setups, we had to interpolate the underlying signal for treadmill and freely walking flies from 180 fps and 150 fps, respectively, to 300 fps (i.e. the tethered setup sampling rate). Finally, a t-test with a Bonferroni correction of 18 was used to determine significant differences between the mean step lengths of freely, treadmill, and tethered walking flies, as well as between control and mechanosensory deficient flies.

A t-test with a Bonferroni correction was also used to compare the means across flies for the following kinematic parameters: bout frequency, forward walking speed, time locomoting, stance distance, stance duration, step speed, probability of the number of legs in stance, and tripod coordination strength. A two-sample Kuiper test (see astropy Python package) was used to statistically compare relative phase distributions. A bootstrap statistical analysis was additionally used to test if there were significant shifts in the mean anterior and posterior extreme positions across the different belt conditions (i.e. tied, slow, and fast belt) of the split-belt task. A Bonferroni correction of 36 was applied (6 legs, 3 belt conditions, and 2 axes of comparison), requiring a $p < 0.0014$ for a significant difference. Note that the kernel density estimations were generated using the seaborn kde function in Python, and that all statistical test were conducted in Python.

KL Divergence for Kinematic Similarity

To determine whether step kinematics of freely walking flies were more similar to those of treadmill or tethered walking flies, we computed the relative KL divergence (Figure S1). KL divergence computes an unbounded similarity, in the form of entropy, between two distributions, where a value closer to zero indicates greater similarity. Thus, we computed the KL divergence between freely and treadmill step kinematic distributions, and freely and tethered distributions. Then, we calculated a relative similarity score between the two sets of distributions by using the following equation:

$$Similarity = 1 - \frac{KL_{freely-treadmill}}{\left(KL_{freely-treadmill} + KL_{freely-tethered}\right)}$$

A value of 1 indicated that freely and treadmill walking step kinematics were more similar than freely and tethered ones, and vice versa.

Kinematic Classification and Quantification

Swing and stance classification

Leg tip velocity was used to classify leg swing and stance phases in all walking setups. We first computed the instantaneous speed of each leg tip from their allocentric positions along the longitudinal and lateral body axes. For the treadmill and tethered walking setups, a rotation matrix had to be applied to the position data to align all flies to a common reference frame and to ensure symmetric contralateral leg movement with respect to the defined axes. The instantaneous speed was then transformed into velocity by applying a negative sign to instances where the leg moved backward along the longitudinal body axis in an egocentric reference frame. This forced the stance to be negative. To achieve this sign application for freely and treadmill walking setups, where the heading of the fly is constantly changing, we rotated the fly in each frame to a common heading. This made it easier to distinguish the period

Please cite this article in press as: Pratt et al., Miniature linear and split-belt treadmills reveal mechanisms of adaptive motor control in walking *Drosophila*, Current Biology (2024), https://doi.org/10.1016/j.cub.2024.08.006

when the leg moved along the body. The instantaneous velocities of the leg tips were then smoothed with a Gaussian kernel. The width of the kernel was chosen such that the signal was not oversmoothed but instantaneous tracking errors were mitigated. Swing was classified as periods where the smoothed leg tip velocities were above and below manually chosen upper (treadmill: 5 mm/s, freely: 15 mm/s, tethered: 0 mm/s) and lower thresholds (all setups: -25 mm/s). Stance was classified as the period where the leg tip velocities were between these thresholds. Finally, we corrected blips in the classification (e.g. converting a swing period consisting of 1 frame into stance) and matched the stance and swing onsets of a given step.

We checked the accuracy of the swing and stance classifications by manually inspecting the raw high-speed videos. Note that we also tried to perform swing and stance classification by thresholding the Hilbert transformed longitudinal body axis position signal of each leg tip, and doing peak detection on that signal, but both methods performed more poorly than the method described above. The Hilbert transform assumes that a signal is non-stationary, which is invalid when using a leg position signal that dynamically moves in 3D. Peak detection also fails to compensate for the richness of leg movement. Overall, our accurate classifications of swing and stance enabled precise quantifications of step kinematics and inter-leg coordination.

Forward walking bout classification

Different forward walking bout classifiers were used for each walking setup, but each captured periods of straight walking (i.e. when heading was stable). In the linear and split-belt setups, forward walking bouts were periods lasting at least 200 ms where the fly walked in the middle of the chamber, had a heading angle within -15 to 15 degrees with respect to the front of the chamber, and had a forward walking velocity (aligned to the driving axis of the treadmill) greater than 5 mm/s. Flies were classified as walking in the middle of the chamber if their abdomen was 1.85 mm in front of the back of the chamber and the tarsi of their front legs were 1.08 mm behind the front of the chamber. Note that for a fly to be considered not walking (i.e. pausing) on the treadmill, it had to be stationary for 150 ms, which was determined by the lack of leg movement. For freely walking flies, the thorax position, specifically the angle between sets of 3 position sample points, was used to first isolate straight body trajectories in allocentric coordinates. A straight trajectory was defined as one where the angles between thorax position sample points were less than 4.5 degrees. Once a straight trajectory was isolated, we classified it as a forward walking bout if the corresponding fly's average body velocity was greater than 5 mm/s, the inter-quartile range of the heading angles was less than 20 degrees, and the duration of the trajectory was greater than 200 ms. Lastly, forward walking bouts of tethered flies were first identified by using a previously described behavioral classifier,[46] but later refined to those greater than 200 ms in duration, having an average forward velocity greater than 5 mm/s, a minimum instantaneous forward velocity of 0.5 mm/s, an average absolute rotational velocity less than 25 degrees/s, and an absolute instantaneous rotational velocity less than 100 degrees/s. Across all setups, the first and last steps of all legs were trimmed within identified forward walking bouts to compensate for the transitions into and out of them.

Forward walking step filtering

Forward walking steps were filtered based on step frequency, stance duration, and swing duration in all walking setups. Forward walking steps were considered to be those that had a step frequency between 5 and 20 steps/s, a swing duration between 15 and 75 ms, and a stance duration less than 200 ms. These filtering thresholds were empirically determined and based on previously published results of forward walking step kinematics in fruit flies.[40,55–57]

Glossary of kinematic parameters

Body length: the distance between the head and distal part of the abdomen.
Body height: the vertical distance between the ground and thorax.
Step frequency: the number of steps completed within a second.
Stance duration: the duration that a leg contacts the ground while walking.
Swing duration: the duration of the aerial phase of leg movement during walking.
Step length: the total distance a leg travels within a step (i.e. stance onset to the subsequent stance onset) in allocentric coordinates.
Stance distance: the total distance (in egocentric coordinates) a leg travels along the longitudinal and medial-lateral body axes within the stance phase of the step cycle.
Step speed: the total distance a leg travels within a step in egocentric coordinates divided by the duration of the step.
Anterior extreme position: the position where a leg first contacts the ground (i.e. stance onset) in egocentric coordinates.
Posterior extreme position: the position where a leg first takes off from the ground (i.e. swing onset) in egocentric coordinates.
Number of legs in stance: the number of legs contacting the ground at a given moment in time.
L1 relative phase: the relative offset in the stance onsets between the left front leg and the leg of interest with respect to the left front leg's step cycle.
Tripod step order: the order in which the legs within a tripod group (i.e. ipsilateral front and hind legs and the contralateral middle leg) first enter stance with respect to the left front leg's step cycle.
Tripod coordination strength: the strength of the coupling between the legs within a tripod as computed by dividing the total time all legs within a tripod overlap during the swing phase of the step cycle, by the total duration of the swing phase for the correspond step (i.e. time between the first leg entering swing and the last leg terminating swing).

Current Biology, Volume *34*

Supplemental Information

Miniature linear and split-belt treadmills reveal mechanisms of adaptive motor control in walking *Drosophila*

Brandon G. Pratt, Su-Yee J. Lee, Grant M. Chou, and John C. Tuthill

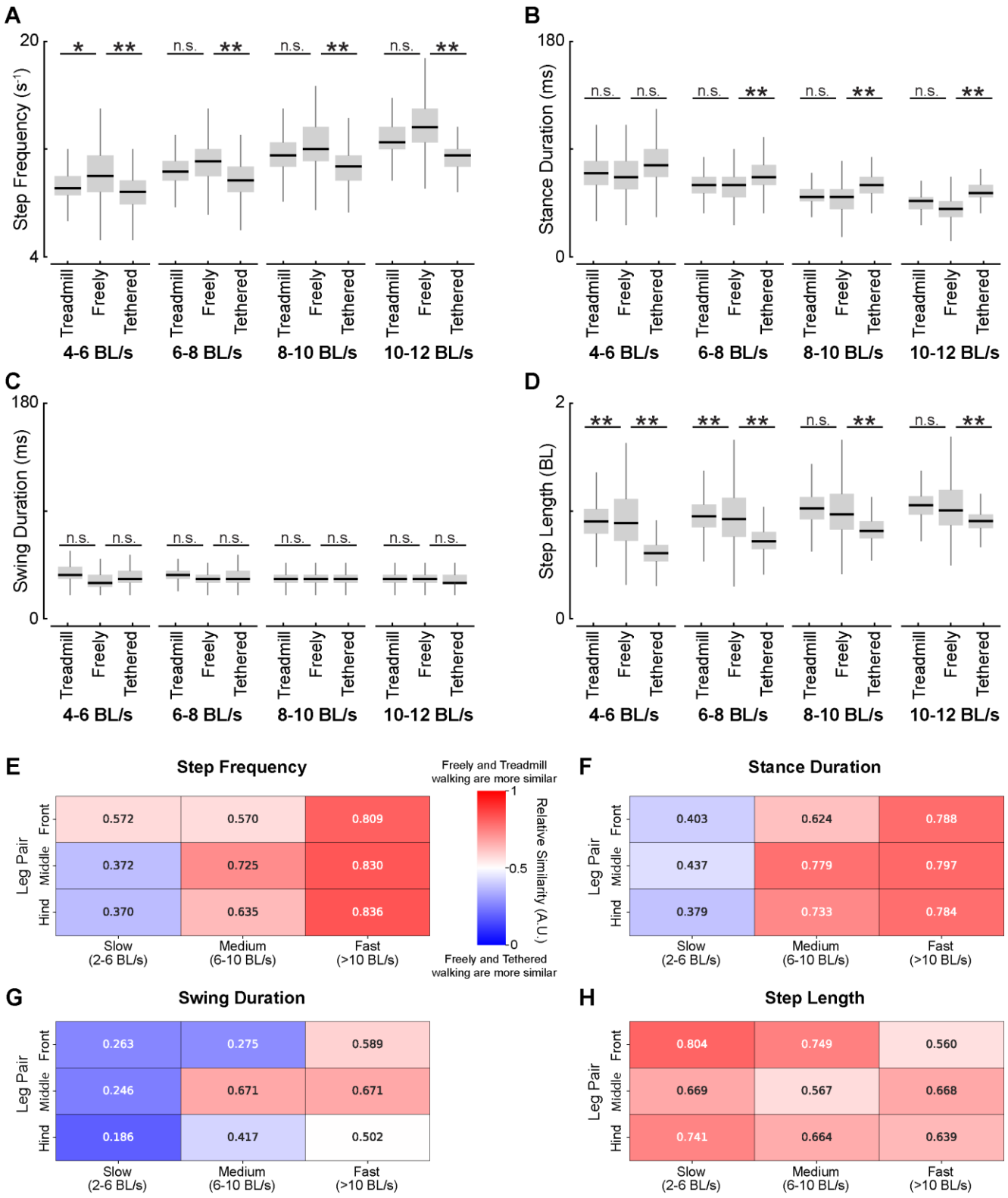

Figure S1. Distributions of step kinematics are more similar between freely and treadmill walking flies than between freely walking and tethered flies, Related to Figure 2. (**A**) Step frequency distributions over the walking speed ranges of 4-6 BL/s, 6-8 BL/s, 8-10 BL/s, and 10-12 BL/s for the treadmill, freely, and tethered walking setups. Chi-squared test for goodness of fit with a Bonferroni correction was used to statistically compare (*: $p < 0.0028$; **: $p < 0.0014$) the distributions of freely walking flies to those of the other walking setups. (**B**) Stance duration distributions over the same walking speed ranges for each walking setup. Chi-squared test for goodness was also used as the statistical test. (**C**) Swing duration distributions over the same walking speed ranges for each walking setup. Chi-squared test for goodness was also used as the statistical test. (**D**) Step

length distributions for each walking speed range and for each walking setup. A t-test with a Bonferroni correction was used to statistically compare (*: $p < 0.0028$; **: $p < 0.0014$) the distributions. (**E**) Step frequency was more similar between treadmill and freely walking flies, especially at medium (6-10 BL/s) and fast (>10 BL/s) walking speeds. At slow (2-6 BL/s) walking speeds, freely and tethered walking step frequencies were more similar. Relative similarity was determined by dividing the KL divergence of freely and treadmill walking kinematic distributions by the sum of the KL divergences between freely and treadmill walking, and freely and tethered walking kinematic distributions. We then reversed the similarity scale by computing 1 minus these values. A value close to 1 indicates that freely and treadmill step kinematics are more similar than freely and tethered walking kinematics for a given walking speed range. The opposite is true for values close to 0. (**F**) Stance duration was more similar between freely and treadmill walking. At slow walking speeds, freely and tethered walking stance durations were slightly more similar than that of treadmill walking. (**G**) Swing duration was more similar between freely and treadmill walking flies at fast speeds, whereas the swing duration of freely and tethered walking flies was more similar at slower speeds. (**H**) Step length was most similar between freely and treadmill walking flies across all speeds and legs.

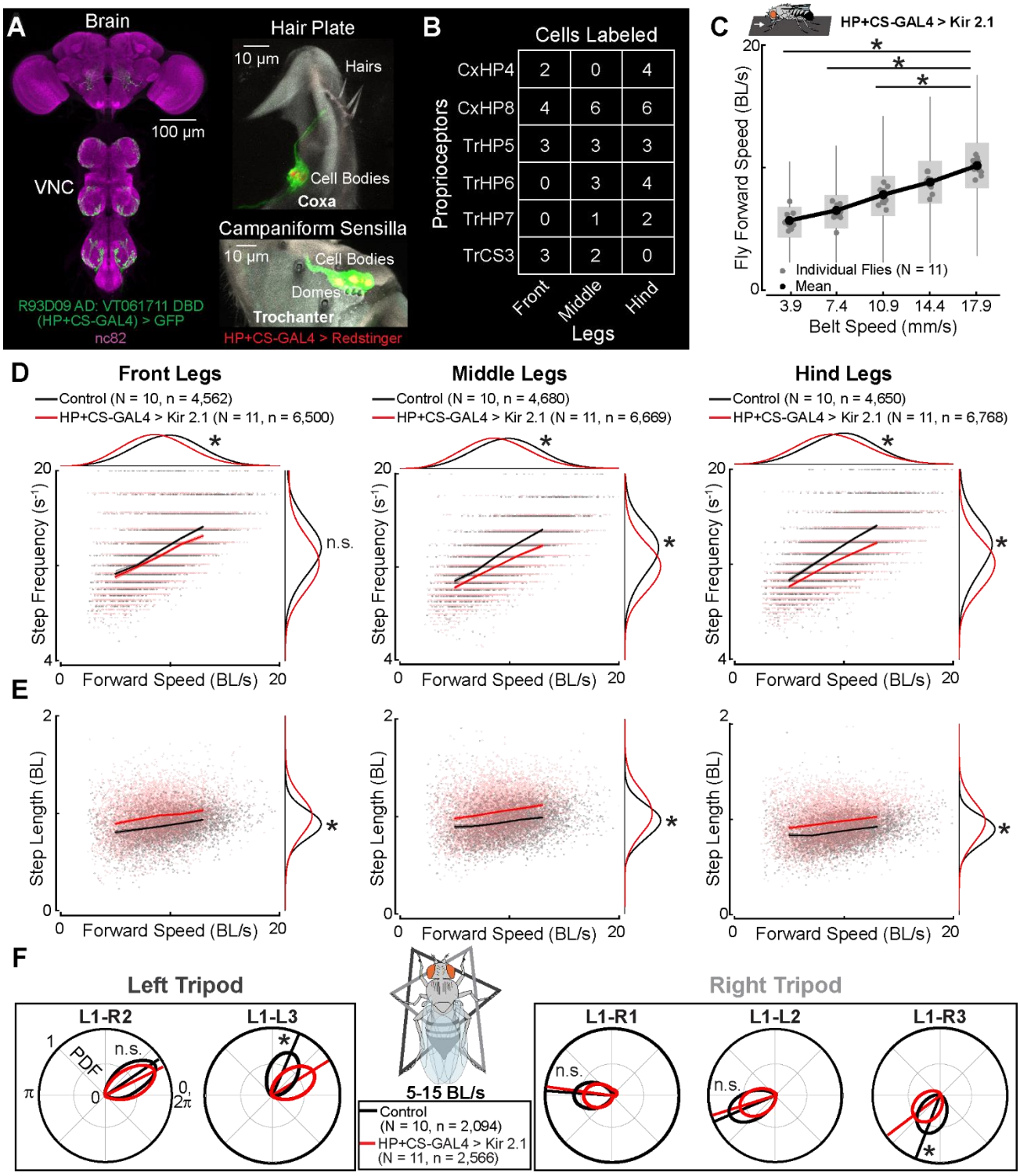

Figure S2. Silencing mechanosensory feedback from hair plates and campaniform sensilla alters step kinematics and slightly influences inter-leg coordination, Related to Figure 4. (**A**) Max intensities projections of confocal stacks of the brain, VNC, and legs show the neurons labeled, including hair plate and campaniform sensilla neurons, by the R93D09 AD: VT061711 DBD split-GAL4 driver line (full genotype in Table 1), referred to as HP+CS-GAL4. GFP: green; nc82: magenta; Redstinger (nuclear marker): red. (**B**) Number of proprioceptor cells labeled on each leg. (**C**) Flies that had the neurons silenced in (B) with Kir 2.1 significantly (t-test; *: $p < 0.05$) increased their forward walking speed as the belt speed increased. N: number of flies. Box plots (box: 25th to 75th percentile; whiskers: 1.5 IQR from lower and upper quartiles) show the distribution of pooled data. Black line connects the mean forward speed for all flies for each belt speed. Gray dots are the median forward speed of each fly. (**D**) Step frequency for the front (left), middle (center), and hind (right) legs was lower, especially at faster walking speeds, in flies lacking

mechanosensory feedback (red) compared to R52A01 DBD > Kir 2.1 (full genotype in Table 1) controls (black). Lines are speed binned averages (2 BL/s bins from 5-14 BL/s) for each kinematic parameter and the 95% confidence interval is shown by the shaded region. The scatter plots of the two genotypes were slightly offset so that each could be visually distinct. Marginal distributions were computed on the original, non-offset distributions. Chi-squared test for goodness of fit with a Bonferroni correction was used to statistically compare (*: $p < 0.025$) each leg pair's step frequency between flies with silenced mechanosensory neurons and controls. A t-test was used to statistically compare (*.: $p < 0.025$) the walking speed distributions between chordotonal neuron silenced flies and controls. N: number of flies, n: number of steps. (**E**) Step length was greater across all walking speeds and legs for flies lacking mechanosensory feedback (red) compared to controls (black). A t-test with a Bonferroni correction was used to statistically compare (*: $p < 0.025$) the step length between flies with silenced mechanosensory neurons and controls. (**F**) The relative phase relationships between the left front leg and each hind leg over the speed range 5-15 BL/s were the only significant differences (*: $p < 0.016$) between flies with silenced hair plate and campaniform sensilla neurons (red) and controls (black). A two-sample Kuiper test with a Bonferroni correction was used to statistically (*: $p < 0.01$) compare the distributions of fly means. The polar distributions integrate to 1 and were determined by a kernel density estimation. Solid lines: average relative phase. N: number of flies; n: number of phase comparisons.

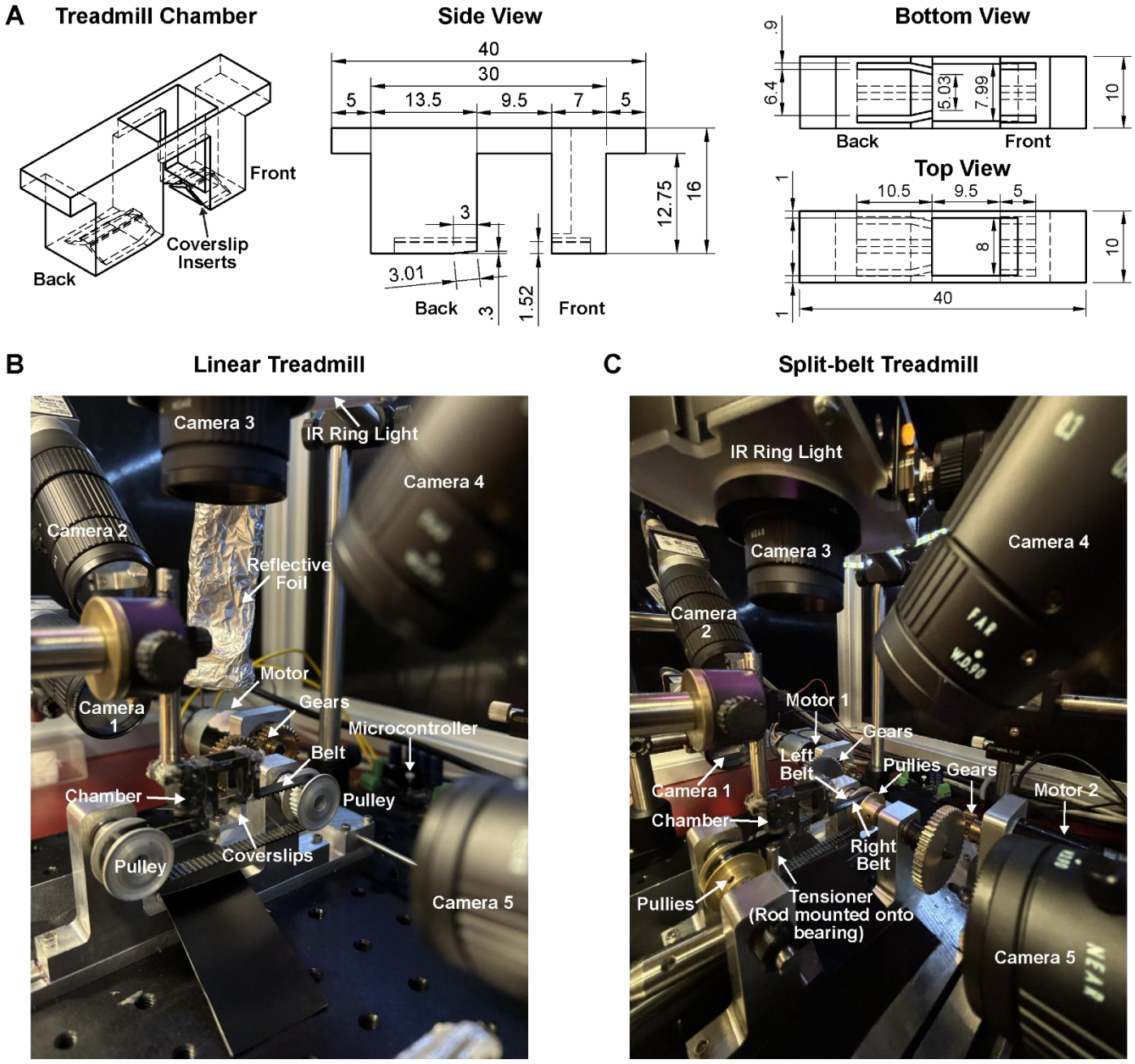

Figure S3. Treadmill chamber and setups, Related to STAR Methods. (**A**) Treadmill chamber schematics made in Autodesk Fusion 360 illustrating the various dimensions of the chamber in millimeters. (**B**) Picture of the linear treadmill system with each component labeled. (**C**) Picture of the split-belt treadmill system with each component labeled.

Kinematics Parameter	Source	Fly Strain	Sex	Mean Value @ 10 mm/s	Mean Value @ 20 mm/s	Mean Value @ 30 mm/s
Step Frequency (s^{-1})	Szczecinski et al., 2018	WT Berlin, Canton S, w^{1118}	Male	9	12.5	15
	Present Study – Treadmill Walking	WT Berlin	Male	9.3	12.1	14.9
	Present Study – Freely Walking	WT Berlin	Male	10	12.6	15.3
	Present Study – Tethered Walking	WT Berlin	Male	9.3	11.5	13.7
Stance Duration (ms)	Szczecinski et al., 2018	WT Berlin, Canton S, w^{1118}	Male	80	50	45
	DeAngelis et al., 2019	WT flies from Gohl et al., 2011	Female	80	50	40
	Mendes et al., 2013	Oregon R	Female	100	60	45
	Present Study – Treadmill Walking	WT Berlin	Male	71	49.3	34.8
	Present Study – Freely Walking	WT Berlin	Male	74.5	48.1	32.6
	Present Study – Tethered Walking	WT Berlin	Male	76.1	53.4	33.2
Swing Duration (ms)	Szczecinski et al., 2018	WT Berlin, Canton S, w^{1118}	Male	35	30	28
	Wosnitza et al., 2013 (data used in above ref.)	WT Canton S	Male	35	30	25
	DeAngelis et al., 2019	WT flies from Gohl et al., 2011	Female	30	35	40
	Mendes et al., 2013	Oregon R	Female	35	32.5	30
	Strauβ and Heisenberg, 1990	WT Berlin	Female	35	30	28
	Present Study – Treadmill Walking	WT Berlin	Male	37.7	34.6	31.3
	Present Study – Freely Walking	WT Berlin	Male	32.1	33.2	34.2
	Present Study – Tethered Walking	WT Berlin	Male	35.5	32.9	30.2
Step Length (mm)	DeAngelis et al., 2019	WT flies from Gohl et al., 2011	Female	1	1.5	2
	Mendes et al., 2013	Oregon R	Female	1.25	1.75	2.25
	Strauβ and Heisenberg, 1990	WT Berlin	Female	1.5	2.25	2.5
	Present Study – Treadmill Walking	WT Berlin	Male	1.87	2.08	2.29
	Present Study – Freely Walking	WT Berlin	Male	2.0	2.25	2.5
	Present Study – Tethered Walking	WT Berlin	Male	1.13	1.72	2.31

Table S1. Summary of previously reported relationships between step kinematics and forward walking speed in *Drosophila melanogaster* and those reported in this study, Related to STAR Methods. Mean values were determined through visual inspection of fits within relevant plots of previous literature. The mean values for the relationships obtained in this study were computed from fits on the data (i.e. linear for step frequency, swing duration, and step length; parabolic for stance duration). The polyfit and polyval functions in python were used to fit the data. Note that the mean values reported for tethered flies at 30 mm/s is estimated from the fits.